Inorganic Chemistry

pubs.acs.org/IC Article

Square-Planar and Octahedral Gyroscope-Like Metal Complexes Consisting of Dipolar Rotators Encased in Dibridgehead Di(triaryl)phosphine Stators: Syntheses, Structures, Dynamic Properties, and Reactivity

Alexander L. Estrada, Leyong Wang, Gisela Hess, Frank Hampel, and John A. Gladysz*

Cite This: *Inorg. Chem.* 2022, 61, 17012−17025 Read Online

ABSTRACT: For a variety of purposes, it is of interest to embed metals in cagelike *trans*-spanning di(triaryl)phosphine ligands. Toward this end, a combination of $P(p\text{-}C_6H_4O(CH_2)_mCH{=}CH_2)_3$ [**3**; m = 4 (**a**), 5 (**b**), 6 (**c**), and 7 (**d**)], $[Rh(COD)(\mu\text{-}Cl)]_2$, and CO gives square-planar *trans*-$Rh(CO)(Cl)[P(p\text{-}C_6H_4O\text{-}(CH_2)_mCH{=}CH_2)_3]_2$ (**4a−4d**). Reactions of **4b−4d** with Grubbs' catalyst (first generation) and then H_2 (catalyst PtO_2) yield the title compounds *trans*-$Rh(CO)(Cl)[P(p\text{-}C_6H_4O(CH_2)_nO\text{-}p\text{-}C_6H_4)_3P]$ ($n = 2m + 2$, **6b−6d**; 26−41% from **4b−4d**). Two are crystallographically characterized. The Cl−Rh−CO moieties rapidly rotate on the NMR time scale at −120 °C, per the ample clearance provided by the $(CH_2)_n$ segments. Steric interactions with the PC_6H_4O linkages are analyzed. LiC≡CAr displaces the chloride ligand from **6b** to give RhC≡CAr adducts (Ar = C_6H_5/p-$C_6H_4CH_3$, **7b**/**8b**). The ArC≡C−Rh−CO rotator of **7b** rapidly rotates on the NMR time scale (−70 °C), but with **8b**, the longer p-$CH_3C_6H_4C{\equiv}C$ group is confined between two $(CH_2)_{12}$ bridges, even at 120 °C. Reactions of $Re(CO)_5(X)$ and **3c** (140 °C) give octahedral *mer,trans*-$Re(CO)_3(X)[P(p\text{-}C_6H_4O(CH_2)_6CH{=}CH_2)_3]_2$ (X = Cl/Br), and metathesis/hydrogenation sequences yield *mer,trans*-$Re(CO)_3(X)[P(p\text{-}C_6H_4O(CH_2)_{14}O\text{-}p\text{-}C_6H_4)_3P]$. Reactions of **6c** and **6d** and excess PMe_3 give the free diphosphines $P(p\text{-}C_6H_4O(CH_2)_nO\text{-}p\text{-}C_6H_4)_3P$ (**14c** and **14d**, 83−75%). The addition of **14d** to $[Rh(CO)_2(\mu\text{-}Cl)]_2$ reconstitutes **6d** (87%). Both *in,in* and *out,out* isomers of **14c** and **14d** are possible, but low-temperature NMR spectra show one set of signals, consistent with rapid homeomorphic isomerizations that turn the molecules inside out. Thermolyses (C_6D_5Br, 140 °C) effect phosphorus inversion to give *in,out* isomers.

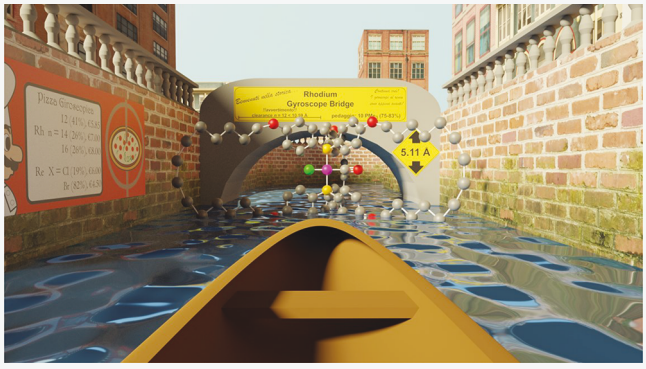

■ INTRODUCTION

Molecular rotors have attracted much recent attention[1] and are commonly dissected into rotators and stators, with the latter assigned to the component with the greater moment of inertia. One particular focus has involved steric shielding of the rotator by the stator.[2−4] Rotating subunits of macroscopic machines are often, although not invariably, confined to protective housings. In the development of molecular machines, it is important to be able to fine-tune the dimensions of any necessary shielding units.

We have had a long-standing interest in the transition-metal-based rotors **II** (Scheme 1), which feature two *trans* phosphorus donor atoms connected by three $(CH_2)_n$ bridges.[5−9] Together these comprise the cagelike stator. Such dibridgehead di(trialkyl)phosphine complexes are usually accessed via 3-fold ring-closing metatheses of square-planar, trigonal-bipyramidal, or octahedral precursors **I**. Typical values of n would be 14, 16, or 18, making for 17-, 19-, or 21-membered macrocycles. The rhodium halide adducts **1** in Scheme 1 (n = 14) are particularly relevant to this study. However, much larger aliphatic systems, such as the platinum dichloride complex **2** with n = 30 and 33-membered macrocycles (Scheme 1), can be accessed.

Throughout this chemistry, the sum of the *trans* P−M−P bond lengths, typically ca. 4.5 Å, constrains the vertical dimensions of the cage. Thus, increasing n will tend to render these assemblies more ovoid, or "fatter" in the horizontal dimension, per the depiction **2**. Also, extended $(CH_2)_n$ segments typically have a range of energetically accessible conformations. It is easy to envision benefits that might accrue from units with

Received: August 9, 2022
Published: October 20, 2022

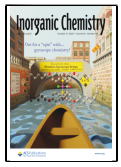

https://doi.org/10.1021/acs.inorgchem.2c02855
Inorg. Chem. 2022, 61, 17012−17025

Scheme 1. Background Reactions and Structures

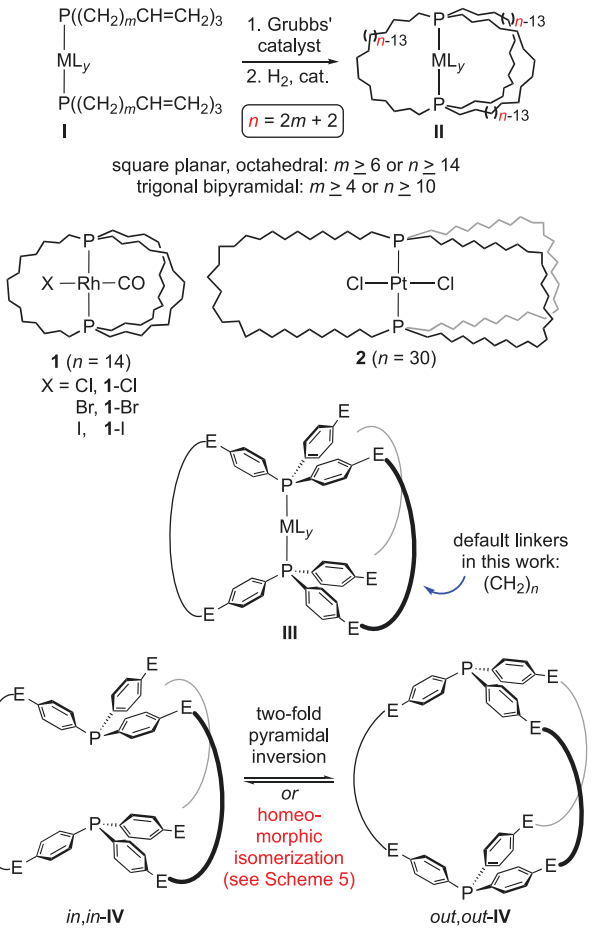

fewer structural degrees of freedom, which might be realized by incorporating "rigid" C≡C or arylene linkages.

Species such as **II** bear some resemblance to common toy gyroscopes and may have applications as molecular gyroscopes.[4] Thus, they are termed "gyroscope-like". Architecturally related silicon-containing systems have been developed by Setaka et al.[3] To engineer more spacious cages, we have been interested in incorporating propeller-like $P(p\text{-}C_6H_4E)_3$ segments[10] into the stators, as shown in **III** (Scheme 1). Would the partially "rigidified" bridges lead to greater "horizontal clearance" or might the nearly linear, *exo*-directed $P-C_{ipso}-C_{para}$ vectors enhance the top/bottom or "vertical clearance"? For most applications, it is important to minimize the rotational barriers of rotators.

Another driving force for this study was the potential for liberating free dibridgehead di(triaryl)phosphines **IV** (Scheme 1) from the metal complexes. There are increasing numbers of avenues for preparing the aliphatic analogues $P((CH_2)_n)_3P$ from **II**,[6,7] including from the rhodium adduct **1**-Cl.[8] As detailed in the Discussion section, there is prior literature on dibridgehead di(triaryl)phosphines and related compounds, all with additional *p*-phenylene moieties in each bridge.[11,12] Importantly, as partially illustrated for **IV**, such compounds can potentially exist as *in,in*, *out,out*, and *in,out* isomers, a separate theme of great interest.[13]

Accordingly, we set out to explore the viability of using ethereal triarylphosphine building blocks of the formula $P(p\text{-}C_6H_4O(CH_2)_mCH{=}CH_2)_3$ to access systems of the type **III**. In this paper, we describe the successful realization of this objective with square-planar rhodium and octahedral rhenium complexes that feature neutral dipolar rotators, properties considered auspicious for the realization of molecular gyroscopes.[1,4] The effective interior dimensions of the stators are mapped through ligand substitutions, NMR experiments, and crystal structures. Also, the viability of **III** as precursors to dibridgehead di(triaryl)phosphines **IV** is demonstrated. A portion of this work has been communicated.[14]

RESULTS

Syntheses of the Title Rhodium Complexes. Bromoarenes with *p*-oxamethylene chains terminating with vinyl groups, $p\text{-}BrC_6H_4O(CH_2)_mCH{=}CH_2$ [*m* = 4 (**a**), 5 (**b**), 6 (**c**), and 7 (**d**)], were prepared by Williamson ether syntheses, as described in the Supporting Information (SI). As shown in Scheme 2, Grignard reagents were subsequently generated, and reactions with PCl_3 gave the triarylphosphines $P(p\text{-}C_6H_4O(CH_2)_mCH{=}CH_2)_3$ (**3a−3d**) in 47−94% yields. These, and all new complexes below, were characterized by NMR (^1H, $^{13}C\{^1H\}$, and $^{31}P\{^1H\}$), IR, microanalyses, and additional physical methods, as summarized in the Experimental Section and the SI.

In a standard procedure,[15] also employed with the trialkylphosphines $P((CH_2)_mCH{=}CH_2)_3$,[8] **3a−3d**, the rhodium chloride complex $[Rh(COD)(\mu\text{-}Cl)]_2$ and CO were combined. As shown in Scheme 2, chromatographic workups gave the bis(phosphine)carbonyl chloride complexes *trans*-$Rh(CO)(Cl)[P(p\text{-}C_6H_4O(CH_2)_mCH{=}CH_2)_3]_2$ (**4a−4d**) as moderately air-stable yellow solids in 49−82% yields. NMR spectra showed the usual ^{103}Rh couplings and also virtual triplets[16] for the PC_6H_4 $^{13}C\{^1H\}$ signals.[8] Key features are illustrated in Figure s8. In lieu of melting point data, representative complexes were characterized by differential scanning calorimetry and thermogravimetric analysis (see the SI).

Next, CH_2Cl_2 solutions of **4a−4d** (ca. 0.001 M) and Grubbs' catalyst (first generation, 15−23 mol % or 5−8%/new C=C linkage) were warmed. Aliquots were periodically assayed by ^1H and $^{31}P\{^1H\}$ NMR. In the case of **4b** and **4c**, chromatography gave the 3-fold ring-closing metathesis products *trans*-$Rh(CO)(Cl)[P(p\text{-}C_6H_4O(CH_2)_mCH{=}CH(CH_2)_mO\text{-}p\text{-}C_6H_4)_3P]$ [*m* = 5 (**5b**) and 6 (**5c**)] in 45% and 49% yields. These feature 25- and 27-membered macrocycles. The $^{31}P\{^1H\}$ NMR spectra of **5b** and **5c** were consistent with (60−50):30:(10−20) mixtures of *Z*/*E* C=C isomers. However, no monorhodium products could be detected from **4a**. In the case of **4d**, the crude product (**5d**) was directly treated with H_2 (5−6 atm) in the presence of PtO_2. As shown in Scheme 2, chromatography gave the target 29-membered macrocycle *trans*-$Rh(CO)(Cl)[P(p\text{-}C_6H_4O(CH_2)_{16}O\text{-}p\text{-}C_6H_4)_3P]$ (**6d**) in 26% overall yield.

Analogous hydrogenations of **5b** and **5c** gave **6b** and **6c** as air-stable yellow solids in 91 and 53% yields, respectively (41% and 26% from **4b** and **4c**, respectively). The NMR spectra of **6b−6d** showed coupling patterns very similar to those of **4a−4d** (e.g., Figure s8). The $^{13}C\{^1H\}$ NMR spectra exhibited a single set of CH_2 signals, even though the $(CH_2)_n$ segments are not symmetry-equivalent in any static structure, the full 360° range of which is shown in Figure s11A. This requires rapid rotation of the Cl−Rh−CO rotators on the NMR time scale.

When $CDFCl_2$[17] solutions of **6b** and **6c** were cooled to −120 °C, $^{13}C\{^1H\}$ and ^1H NMR spectra showed no decoalescence, although peaks severely broadened. Also, the PC_6H_4 moieties

https://doi.org/10.1021/acs.inorgchem.2c02855
Inorg. Chem. 2022, 61, 17012−17025

Scheme 2. Syntheses of Gyroscope-Like Rhodium Complexes Based on Triarylphosphines

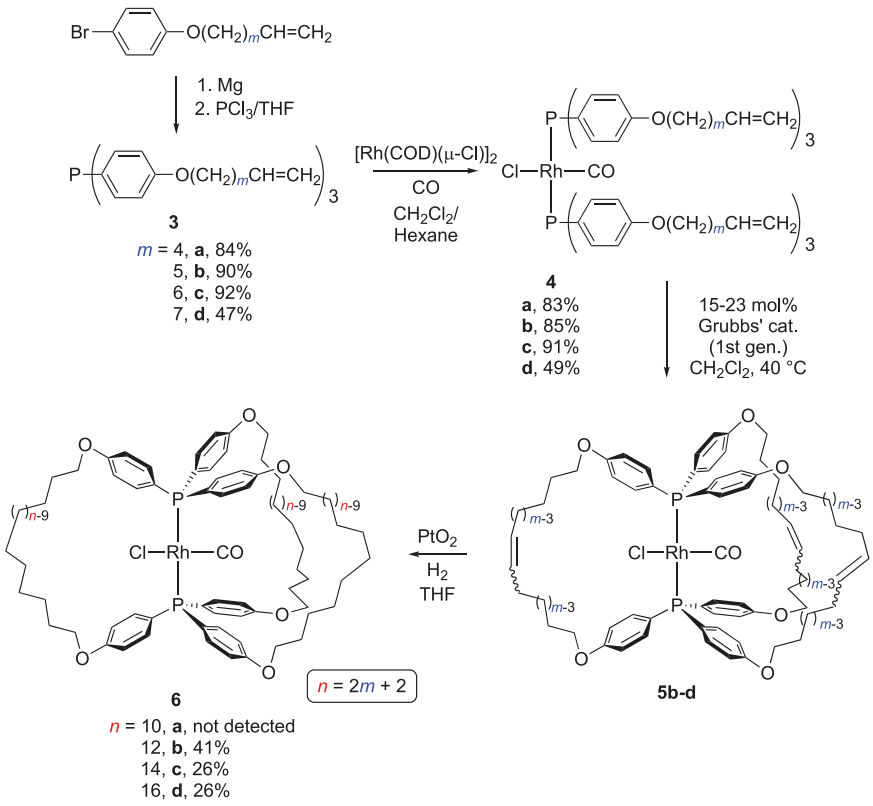

exhibited only two CH $^{13}C\{^1H\}$ and ^1H signals (o and m), indicating rapid oscillation about the P−C_6H_4 bonds, interconverting propeller configurations.[10] Importantly, the $^{31}P\{^1H\}$ and CO $^{13}C\{^1H\}$ signals remained coupled to ^{103}Rh at room temperature, excluding mechanisms involving phosphine or CO dissociation for rendering the CH_2 $^{13}C\{^1H\}$ NMR signals equivalent.

Crystallography. Crystals of the solvates **6b**·$(C_6H_6)_{1.5}$·$(H_2O)_{0.5}$ and **6c**·$(C_6H_6)_{1.5}$·(CH_3OH) could be obtained, and the X-ray structures were determined as outlined in Table s1 and the Experimental Section. Key bond lengths and angles are provided in Figure 1, and torsion angles are summarized in Tables s2 and s3. The metrical parameters and molecular structures, given as both thermal-ellipsoid and space-filling representations in Figure 1, are quite similar. The Rh−P bond lengths (2.32−2.33 Å) and P−Rh−P bond angles (176−179°) translate to P−P distances of 4.648−4.657 Å. Interestingly, the C_{ipso}−P−P−C_{ipso} moieties are nearly eclipsed (torsion angles 4.8−7.6°), with the opposing PAr_3 groups exhibiting mirror image (*meso*) propeller chiralities.

Space-filling **V** and **VI** vividly illustrate the enhanced "horizontal clearance" provided by the dibridgehead di(triaryl)phosphine stators. The distances from the rhodium atoms to the distal methylene carbon atoms are 10.24−10.72 and 10.46−12.05 Å, respectively. When the van der Waals radius of an sp^3 carbon atom (1.70 Å) is subtracted,[18] void distances of at least 8.50 Å remain. These can be compared to the effective radius of the Cl−Rh−CO rotator, 4.46 Å, which is obtained by adding the van der Waals radius of oxygen (1.52 Å) to the RhCO distances (2.939−2.942 Å). The sum of the Rh−Cl bond distances (both 2.365 Å) and the van der Waals radius of chlorine (1.75 Å) is somewhat lower (4.12 Å).

In the crystal lattices, **6b** and **6c** pack with parallel P−Rh−P axes. The benzene molecules tend to be in the vicinity of a macrocycle but not intercalated. For example, **6c** exhibits a benzene/benzene CH/π interaction[19] of 3.8 Å that passes through a macrocycle. The stators in **6b** and **6c** are clearly more porous than those of the well-studied adducts of the dibridgehead di(trialkyl)diphosphine $P((CH_2)_{14})_3P$,[5,6a,8,9] but neighboring rhodium complexes do not intrude into the macrocycle cavities. Thus, the crystals show notably more voids, as evidenced by the much lower densities of **6b** and **6c** (1.173−1.194 Mg m^{-3}, enhanced by solvate molecules) compared to the crystalline rhodium halide complexes **1**-Br and **1**-I (Scheme 1; 1.249−1.300 Mg m^{-3}, with no solvate molecules).

The representations **VII** and **VIII** highlight the relationships of the macrocycles in neighboring molecules. Two are quite closely nestled in each case. The closest intermolecular Rh−C distances are 4.84 and 4.80 Å, respectively (Figure s1), which after subtraction of the van der Waals radius of carbon give clearances of 3.14−3.10 Å. Considering the radius of the Cl−Rh−CO rotator (4.65 Å; *vide supra*), rotation should be severely impeded in the solid state. However, for trigonal-bipyramidal adducts of $P((CH_2)_{14})_3P$ with small ligands such as CO, NO, CN, or halides, rotators can, in principle, rotate in the solid state without steric interactions with neighboring molecules.[4,5,9a]

Substitution Reactions and Additional Dynamic Properties. Attention was turned to "braking" the rotation of rotators within the dibridgehead di(triaryl)phosphine stators. Rhodium chloride complexes *trans*-Rh(CO)(Cl)$(L)_2$ have been shown to undergo substitution by acetylide nucleophiles.[20] Furthermore, the van der Waals radii of acetylide ligands are easily varied. Thus, as shown in Scheme 3, **6b** and LiC≡CC_6H_5 were combined in tetrahydrofuran (THF). The $^{31}P\{^1H\}$ NMR spectra of aliquots showed a nearly quantitative conversion.

https://doi.org/10.1021/acs.inorgchem.2c02855
Inorg. Chem. 2022, 61, 17012−17025

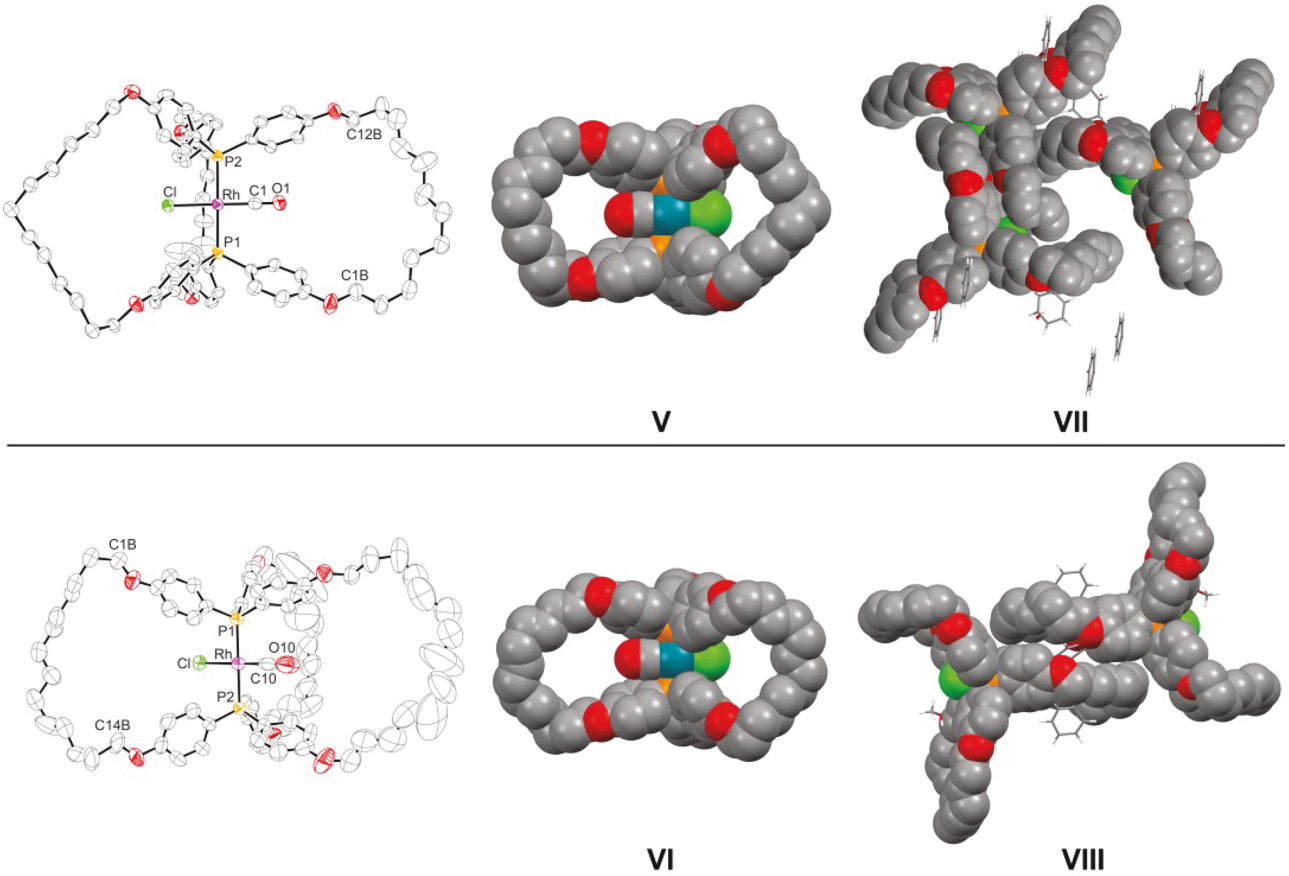

Figure 1. Thermal-ellipsoid (50% probability) and space-filling representations of the crystal structures of **6b**·$(C_6H_6)_{1.5}$·$(H_2O)_{0.5}$ (top) and **6c**·$(C_6H_6)_{1.5}$·(CH_3OH) (bottom). The solvent molecules are included in **VII** and **VIII**. Key bond lengths (Å) and angles (deg): Rh−P1 2.322(1)/2.325(2), Rh−P2 2.329(1)/2.333(2), Rh−CO 1.790(5)/1.79(1), C−O 1.154(7)/1.15(1), Rh−Cl 2.365(1)/2.365(2); P1−Rh−P2 175.87(4)/179.26(6), P1−Rh−C 91.0(2)/90.6(3), P2−Rh−C 89.8(2)/89.7(3), P1−Rh−Cl 88.18(4)/89.02(5), P2−Rh−Cl 91.38(4)/90.67(6), C−Rh−Cl 174.7(2)/178.0(3), Rh−C−O 176.4(5)/178.7(9).

Scheme 3. Substitution of the Chloride Ligand in Gyroscope-Like Rhodium Complex 6b

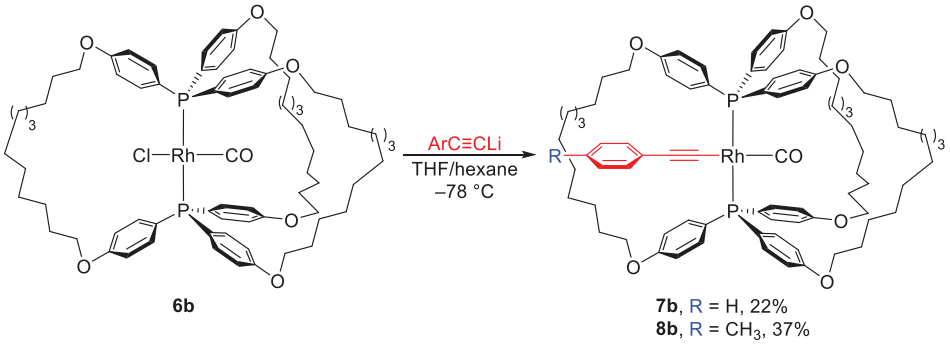

Workup gave the dark-yellow phenylacetylide complex **7b**, which was somewhat labile in all solvents investigated, in 22% yield.

The NMR properties of **7b** and IR $\nu_{CO}/\nu_{C\equiv C}$ values (1976/2239 cm^{-1}, s/w) were similar to those of the triphenylphosphine analogue *trans*-Rh(CO)(C≡CC_6H_5)(PPh_3)$_2$.[21] In the reported crystal structure,[21] the distance from rhodium to the *p*-carbon atom of the phenyl ring is 7.38 Å. When the van der Waals radius of carbon is added, the radius of the rotator becomes comparable to the horizontal clearance offered by the stator in **6b** (9.08 vs 8.54−9.02 Å). However, $^{13}C\{^1H\}$ NMR spectra of **7b** in CD_2Cl_2 at −70 °C showed only one set of six CH_2 signals for all three bridges, indicating rapid rotation of the $C_6H_5C\equiv C-Rh-CO$ moiety on the NMR time scale.

To augment the radius of the rotator, a similar reaction was conducted with the *p*-tolylacetylide LiC≡C-*p*-$C_6H_4CH_3$. This gave the corresponding complex **8b** (37%, Scheme 3), for which the distance from rhodium to the *p*-methyl carbon can be estimated as 8.89 Å (7.38 Å + 1.51 Å for C_{sp^2}-CH_3). The corresponding van der Waals radius (10.59 Å) is now distinctly greater than the clearance offered by the stator. As illustrated in Figure 2, NMR spectra in CD_2Cl_2 at room temperature showed two distinct types of bridges. Two sets of six CH_2 $^{13}C\{^1H\}$ signals, as well as two sets of P$\underline{C_6H_4}$ $^{13}C\{^1H\}$ and ^1H signals,

https://doi.org/10.1021/acs.inorgchem.2c02855
Inorg. Chem. 2022, 61, 17012−17025

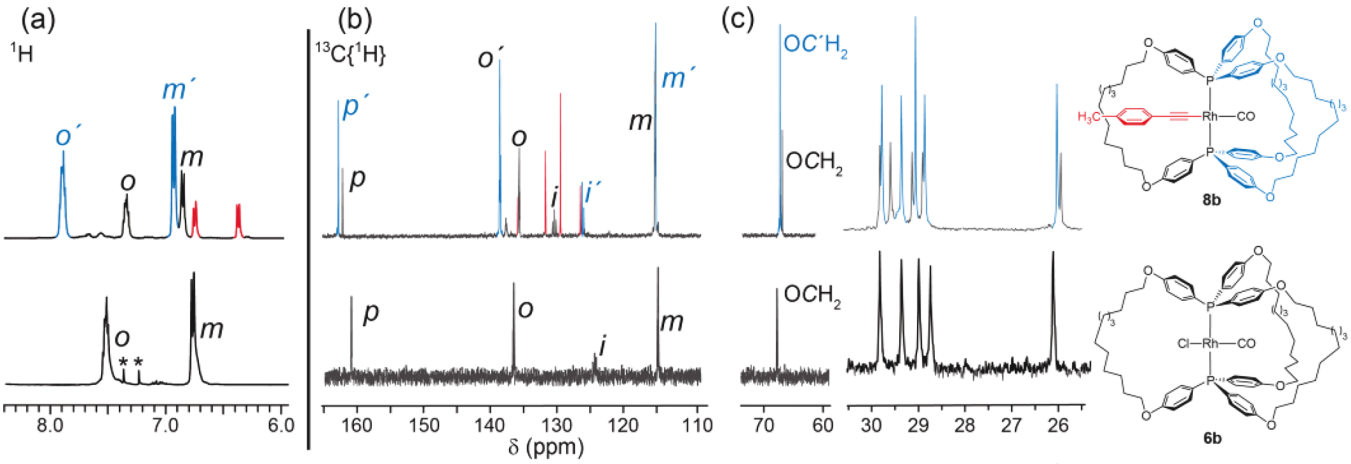

Figure 2. NMR spectra of **8b** (top, CD_2Cl_2) and **6b** (bottom, $CDFCl_2$, −20 °C): (a) ^{1}H (400 MHz), aryl region; (b and c) $^{13}C\{^1H\}$ (100 MHz). Signals associated with the solvent or impurities are marked by asterisks. The aryl signals of the $C_6H_4CH_3$ group are depicted in red but not assigned.

were detected, all in ca. 2:1 area ratios (Figure 2a,b). These features persisted in spectra recorded in C_6D_5Cl at 120 °C, under which conditions **8b** began to decompose. The two H_{ortho} ^{1}H NMR signals could be used to conservatively bound the $\Delta G^{\ddagger}_{363\ K}$ value for rotation as >17.5 kcal/mol.[22]

As shown in Figure 3, the NMR data for **8b** can be modeled by a rapid equilibrium involving the rotamers **IX** and **X** and the transition state **XI**.[23] This entails passage of the shorter CO ligand through the macrocycle labeled A, a process that must be facile given the rapid Cl−Rh−CO rotation in **6b**−**6d**. The longer C≡C-*p*-$C_6H_4CH_3$ ligand remains confined within a <120° arc bordered by the two macrocycles B and B′. This results, on a time-averaged basis, in two types of bridges and aryl rings per the two sets of NMR signals with 2:1 area ratios. If neither of the two rhodium ligands could pass through a macrocycle, three sets of signals would be expected. Additional graphical representations of these limits are provided in Figure s11.

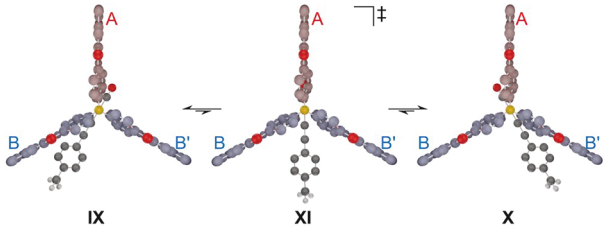

Figure 3. Mechanism for rendering two of the three bridges in **8b** equivalent.

Syntheses of the Title Rhenium Complexes. It was sought to extend the ring-closing metatheses in Scheme 2 to other coordination geometries. Reactions of octahedral rhenium pentacarbonyl halides and phosphines (2 equiv) can give either *fac* or *mer,trans* disubstitution products, but the latter generally dominates at sufficiently elevated temperatures.[9b,24] As shown in Scheme 4, $Re(CO)_5(Cl)$[25] and **3c** (2.3 equiv) were combined in chlorobenzene at 140 °C. Workup gave the target complex *mer,trans*-$Re(CO)_3(Cl)[P(p\text{-}C_6H_4O(CH_2)_6CH{=}CH_2)_3]_2$ (**10c**) as a yellow oil in 57% yield. The corresponding reaction of $Re(CO)_5(Br)$[25] and **3c** gave the analogous bromide complex **11c** (69%).

Scheme 4. Syntheses of Gyroscope-Like Rhenium Complexes Based upon Triarylphosphines

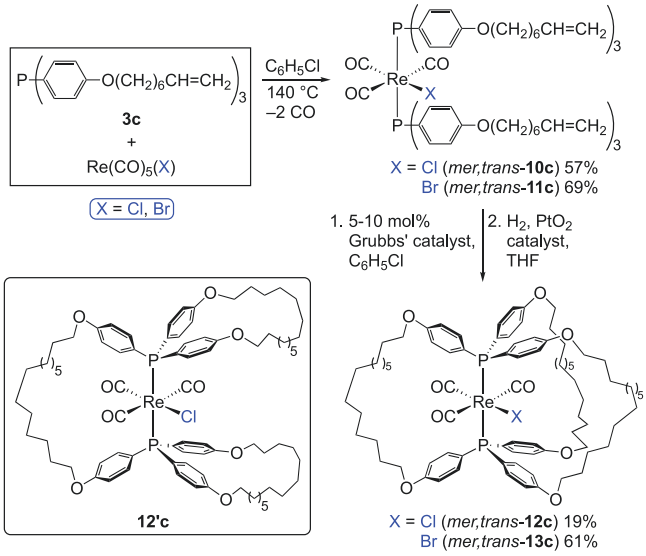

The *mer* relationships of the carbonyl ligands were evidenced by the IR ν_{CO} patterns,[26] and the *trans* relationships of the phosphine ligands were, in turn, indicated by the single $^{31}P\{^1H\}$ NMR signals. Accordingly, the $^{13}C\{^1H\}$ NMR spectra exhibited two triplets (2:1) for the carbonyl ligands. Similar patterns have been previously observed for comparable complexes, including analogues with trialkylphosphine ligands $P((CH_2)_mCH{=}CH_2)_3$.[9b,24c,27]

As depicted in Scheme 4, ring-closing metatheses were carried out similarly to those in Scheme 2 but using dilute chlorobenzene solutions (0.0011 M) and 5−10 mol % catalyst. The less volatile solvent facilitated aspiration of nitrogen through the mixture to remove the ethylene coproduct. The crude metathesis products, which exhibited four principal $^{31}P\{^1H\}$ NMR signals, were treated with H_2 (balloon pressure) in the presence of PtO_2. Chromatographic workups gave the target 27-membered macrocycles *mer,trans*-$Re(CO)_3(X)[P(p\text{-}C_6H_4O(CH_2)_{14}O\text{-}p\text{-}C_6H_4)_3P]$ [X = Cl (**12c**) and Br (**13c**)] as air-stable white powders in 19% and 61% overall yields.

https://doi.org/10.1021/acs.inorgchem.2c02855
Inorg. Chem. 2022, 61, 17012−17025

Scheme 5. Displacement and Reinsertion of the Cl−Rh−CO Rotator from/into the Dibridgehead Di(triaryl)phosphines 14c and 14d

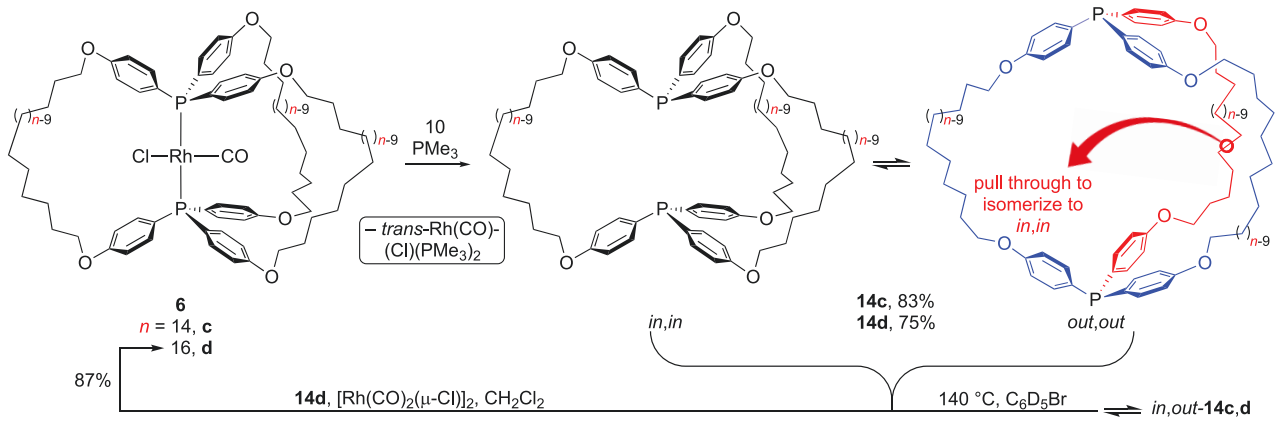

Attempts to similarly access the 23-membered analogue **12a** from the $(CH_2)_4$ species **10a** are detailed in the SI. While **10a** was easily prepared, the macrocycle was not obtained in spectroscopically pure form. Also, some syntheses of **12c** gave a second (separable) product, but this was not reproducible. In this context, an isomer of **12c**, derived in part from *intra*ligand metathesis, is depicted in Scheme 4 (**12′c**). Although such species are definitely not the major products of any reactions reported herein, there is always the possibility that minor quantities were lost upon workup or otherwise escaped attention. Adducts of this type *were* isolated in reactions of analogous rhenium complexes containing trialkylphosphine ligands $P((CH_2)_mCH{=}CH_2)_3$.[9b]

The octahedral complexes **12c** and **13c** have rotators consisting of four ligands, as opposed to two in the square-planar rhodium complexes. Nonetheless, the radius-determining ligand is again CO, as taken from crystallographic distances for the corresponding complexes with aliphatic $P(CH_2)_{14}P$ bridges (4.55−4.63 Å for ReCO vs 4.28 or 4.51 Å for the chloride or bromide ligands).[9b] Accordingly, only a single set of CH_2 $^{13}C\{^1H\}$ NMR signals was observed, indicating rapid Re(CO)$_3$(X) rotation on the NMR time scale, as seen with $P(CH_2)_{14}P$ bridges.[9b] Representative $^{13}C\{^1H\}$ NMR data are shown in Figure s9.

Dibridgehead Di(triaryl)phosphines. To conclude this study, liberation of the dibridgehead di(triaryl)phosphine ligands from the rhodium complexes **6b** and **6c** was investigated. The aliphatic diphosphine $P((CH_2)_{14})_3P$ can be displaced from the rhodium chloride complex **1**-Cl with excess PMe_3.[8] However, in view of a mechanistic hypothesis in the Discussion section, there was concern that the "rigidity" of the *p*-phenylene groups in **6b** and **6c** might prove problematic.

As shown in Scheme 5, **6c** and **6d** were treated with excess PMe_3. Chromatographic workups gave the target diphosphines $P(p\text{-}C_6H_4O(CH_2)_nO\text{-}p\text{-}C_6H_4)_3P$ (**14c** and **14d**; n = 14 and 16) as white solids in 75−83% yields. The $^{31}P\{^1H\}$ NMR signals (ca. −5 ppm) shifted markedly upfield from those of **6c** and **6d** (ca. 25 ppm), and virtual and rhodium couplings vanished from the ^1H and $^{13}C\{^1H\}$ NMR signals. Mass spectra showed the expected molecular ions.[28] The well-known PMe_3 complex *trans*-Rh(CO)(Cl)$(PMe_3)_2$[29] formed concurrently, as assayed by $^{31}P\{^1H\}$ NMR, and PEt_3 reacted similarly.

As noted in Scheme 1, dibridgehead di(triaryl)phosphines such as **14c** and **14d** can exist as *in,in*, *out,out*, and *in,out* isomers. In the complexes **6b**−**6d**, both phosphorus lone pairs are locked into *in* positions. When decomplexed, the diphosphines can, in principle, turn themselves inside out to *out,out* isomers by a topological process ("homeomorphic isomerization"),[30] which is not widely appreciated but is well documented for the aliphatic analogues $P((CH_2)_n)_3P$[31] and some species with carbon bridgeheads.[32] This entails pulling one $p\text{-}C_6H_4O\text{-}(CH_2)_nO\text{-}p\text{-}C_6H_4$ segment through the macrocycle defined by the other two, per the bold red arrow in Scheme 5. The barriers are often low, but in smaller macrocycles, a slow exchange limit can sometimes be reached. With the aliphatic analogues, it is possible to observe two $^{31}P\{^1H\}$ NMR signals (unequal ratios) for $n \leq 14$.[31] However, when solutions of **14c** and **14d** were cooled (toluene-d_8), only broadened signals were observed.

As shown in Scheme 5, a CH_2Cl_2 solution of **14d** was treated with $[Rh(CO)_2(\mu\text{-}Cl)]_2$. Under conditions analogous with those of the aliphatic diphosphine $P((CH_2)_{14})_3P$, the Rh(CO)(Cl) fragment was reintroduced between the phosphorus atoms, (re)generating **1**-Cl.[7,8] Accordingly, **6d** reformed in quantitative spectroscopic yield, or 87% yield after workup.

As a final probe of the stereoisomerism, C_6D_5Br solutions of **14c** and **14d** were kept at 140 °C. Such conditions usually effect the pyramidal inversion of phosphines.[31,33] $^{31}P\{^1H\}$ NMR monitoring revealed a new signal that could plausibly be assigned to an *in,out* isomer (Figure s10).[28] However, in some experiments, species with plausible chemical shifts for phosphine oxides grew in at slightly slower rates, complicating preparative extensions. Certain phosphines are plagued by oxidations under seemingly anaerobic conditions, whereas others are stable for extended periods in air.[34]

■ DISCUSSION

Syntheses. This study has established the ready availability of a special class of gyroscope-like complexes, sometimes termed "giant",[14] based upon dibridgehead di(triaryl)phosphine ligands (Schemes 2 and 4). The overall yields for the 3-fold metathesis/hydrogenation sequences appear, on average, to be slightly lower than those for dibridgehead di(trialkyl)phosphines. Perhaps the triaryl systems are more disposed toward intermolecular metathesis, leading to oligomers or polymers that might be poorly soluble or retained on chromatographic supports.

At present, there does not appear to be an upper limit on the ring sizes of macrocycles **6**, which reach 29 atoms in the case of **6d**. However, this is not the "record" when all types of bridges are considered because the di(trialkyl)phosphine complex **2** (Scheme 1) features 33-membered rings. For the di(triaryl)-

https://doi.org/10.1021/acs.inorgchem.2c02855
Inorg. Chem. 2022, 61, 17012−17025

phosphine adducts, the routes in Schemes 2 and 4 appear to have practical lower limits of 25-membered macrocycles (n = 12), although in the rhenium series, the 23-membered homologue was at least detectable, as detailed in the SI.

For all classes of diphosphine ligands, we find the synthetic success with octahedral precursors (Scheme 4) surprising. During the metathesis step, the six $X(CH_2)_nCH{=}CH_2$ segments must find their way through an equatorial plane with four ligands. This would seemingly disfavor interligand metathesis, leading to (besides oligomers) species such as **12′c** in Scheme 4. These have sometimes been observed with other square-planar and octahedral systems[6b,8] but are almost always minor products.

2. Stator Dimensions and Dynamic Properties. Any estimation of the "horizontal clearance" afforded by the stators in gyroscope-like complexes is approximate because many conformations are available and several approaches to defining the distal carbon atoms are possible. Nonetheless, it would seem possible to engineer still greater clearances than those in **6b** (10.24−10.72 Å) or **6c** (10.46−12.05 Å) by introducing additional methylene groups or *p*-phenylene moieties to the bridges. For comparison, values of 5−6 Å have been calculated for $P((CH_2)_{14})_3P$ stators in the crystalline rhodium halide complexes **1**-Br and **1**-I and a host of related platinum and palladium adducts.[6a,8] This renders the rotation of Ph−Pt−Ph or SCN−Pt−NCS rotors slow on the NMR time scale at room temperature

In some studies, we have also analyzed the top/bottom or "vertical clearance",[5,8,22b] which is always a tighter fit with respect to the steric demands of the ligands on the rotator (e.g., the van der Waals diameter of a radially symmetric ligand). One approach to enhancing the vertical clearance is to replace phosphorus by arsenic, which increases the bond lengths to the metal by ca. 4%.[7,22b] Accordingly, rotational barriers drop by several kilocalories per mole.[22b] Because most rotators of interest to date have relatively modest radii, distances associated with the first few atoms bound to each phosphorus (or arsenic) atom are of the greatest interest.

The representations in Figure 4 are used to compare the vertical clearances of the dibridgehead di(triaryl)phosphines (**XII**, top) and aliphatic analogues (**XIII**, bottom). As noted earlier, the P−C_{ipso}-C_{para} vectors in **6b**−**6d** are angled away from (or *exo* to) the plane of the rotator, which is auspicious for reduced interactions. However, the *o*- and *m*-carbon atoms angle back toward the rotator, with the degree dependent upon the propeller tilt of the ligand. Regardless, the average distances for the first five atoms bound to phosphorus in **6b** and **6c** are 3.069, 2.553, 3.046, 4.058, and 4.569 Å, respectively.

As illustrated in the inset in Figure 4, complexes of dibridgehead di(trialkyl)phosphines can exhibit two limiting M−P−CH_2−CH_2 conformations, **XIII-B** (*gauche*) and **XIII-A** (*anti*). In crystal structures that feature six such segments, the former always dominate, and those of **1**-Br and **1**-I exhibit a single *anti* linkage (vs five *gauche*). In any case, the average distances from the plane of the rotator for the first carbon atom are very close (3.085 vs 3.069 Å). For the second and third atoms, the distances are greater for the trialkylphosphines (2.942 vs 2.553 Å and 3.359 vs 3.046 Å), although the differences narrow by ca. 0.3 Å if the *anti* segment **XIII-A** is excluded. However, for the fourth and fifth atoms, the distances are much greater for the triarylphosphines (4.058 vs 2.835 Å and 4.569 vs 2.508 Å).

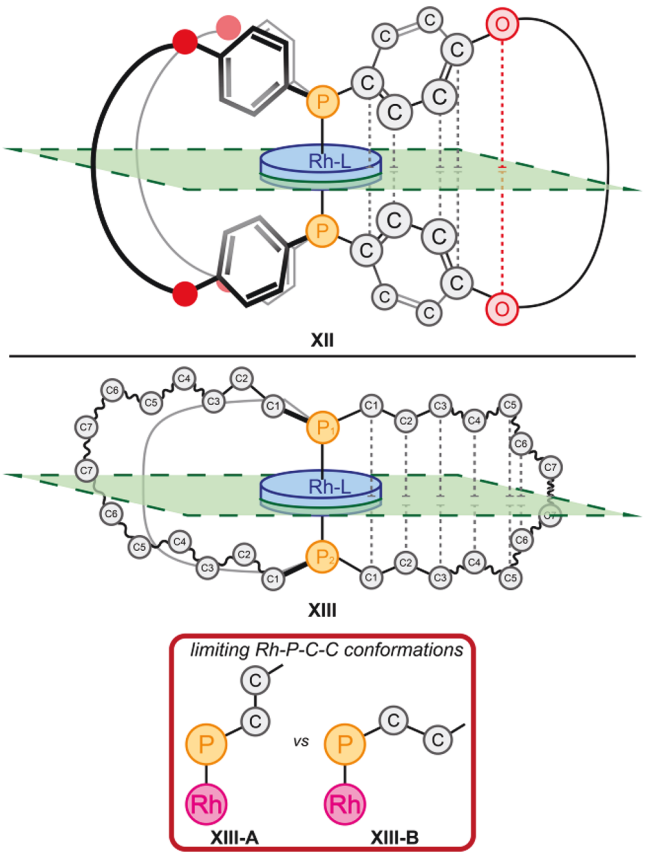

Figure 4. Top (**XII**): Distances of atoms of the dibridgehead di(triaryl)phosphine ligands in **6b** and **6c** from the rotator planes (Å, averages of 12 values): C_{ipso} 3.069, C_{ortho}(*endo*) 2.553, C_{meta}(*endo*) 3.046, C_{para} 4.058, O 4.569. Bottom (**XIII**): Distances of the atoms of dibridgehead di(trialkyl)phosphine ligands from the rotator planes. Average of 12 values for **1**-Br and **1**-I (Å): C1 3.085, C2 2.942, C3 3.359, C4 2.835, C5 2.508.

Thus, it is challenging to assess the more favorable type of cage with respect to vertical steric interactions with the rotator. Another factor is that any motion of the rotator is logically correlated to conformational changes in the macrocycle. Despite the shorter distances for C_{ortho} and C_{meta} in **XII**, these can be viewed as part of a "swinging gate", whereas C1 and C2 in **XIII** are closer to "hard barriers". The optimum choice can also be rotator-dependent. For example, the triarylphosphines are better fits for ligands such as C≡C*t*-Bu, where the steric demand increases with the distance from the axis. In any case, we view the triarylphosphines as equal or better than the trialkylphosphines with respect to vertical clearance.

Finally, we compare the steric demands of the Cl−Rh−CO rotators in **6b** and **6c** with the "vertical clearance". The van der Waals diameter of the chloride ligand is 3.50 Å, and those of the carbon and oxygen atoms that comprise the CO ligand are 3.40 and 3.04 Å, respectively. Hence, the chloride ligand is "thickness determining". To estimate the vertical clearance, the distances of C_{ipso}, C_{ortho}, and C_{meta} from the rotator planes are doubled, and twice the van der Waals radii of the sp^2 carbon atoms is subtracted. This gives void spaces of 2.74, 1.71, and 2.69 Å, respectively, all considerably smaller than 3.50 Å. Hence, rotation must be accompanied by considerable steric interactions, ameliorated to some degree by simultaneous conformational adjustments of the stator.

https://doi.org/10.1021/acs.inorgchem.2c02855
Inorg. Chem. 2022, 61, 17012−17025

Scheme 6. Speculation Regarding the Substitution Mechanisms in Schemes 3 and 5

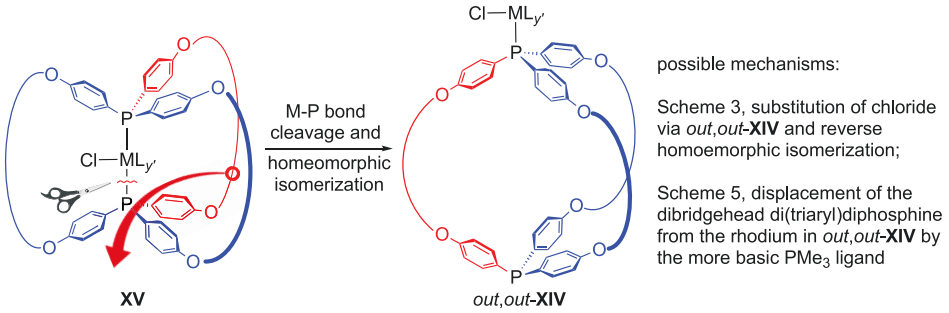

Additional Mechanistic Issues. Several mechanistic issues attend the chloride and di(triaryl)phosphine ligand substitution reactions in Schemes 3 and 5. From the crystal structures in Figure 1, the chloride ligand appears to be reasonably accessible for displacement. However, chloride substitution also occurs readily in more congested dibridgehead diphosphine complexes,[6a,8] such as the $P((CH_2)_{14})_3P$ adduct **1**-Cl (Scheme 1).[8] Accordingly, we have previously suggested that such processes may occur by the initial metal−phosphorus bond cleavage, followed by homomorphic isomerization. For the complexes in this study, this would afford species of the type *out,out*-**XIV** in Scheme 6.

This generates a more open environment for chloride ligand substitution. It also provides a more favorable environment for displacement of the dibridgehead di(triaryl)phosphine by more basic donor ligands, such as PMe_3. Alternatively, a phosphine-free rhodium(I) source such as $[Rh(CO)_2(\mu\text{-Cl})]_2$ could combine with the *out,out* isomer of the free diphosphine to give *out, out*-**XIV** and then, via homeomorphic isomerization, **XV**.

As noted in the Introduction, the dibridgehead di(triaryl)-diphosphine ligands were designed to be partially "rigidified" compared to the aliphatic homologues. As conformational degrees of freedom or flexibility diminish, activation barriers for homeomorphic isomerizations should increase. However, isomerization appears to remain facile in the ligand systems studied to date. There is a strong impetus to introduce further steric constraints, connected to numerous reactions that can be catalyzed by rhodium(I) species. For example, new or improved selectivities are possible when catalysis is constrained to occur within confined spaces.[35] However, equilibria involving species such as *out,out*-**XIV** open up catalytic pathways that would be external to the cagelike ligand.

Dibridgehead Di(triaryl)phosphines. Compounds **14** are not the first dibridgehead di(triaryl)phosphines to be reported. In a landmark study, Bauer et al.[12] reported the surprisingly successful 3-fold Williamson ether syntheses of the dibridgehead di(triaryl)phosphine dioxides **16**·2O shown in Scheme 7. This sequence is likely facilitated by the dimethylated quaternary carbon atoms and the Thorpe Ingold effect.[36] Both the *in,in/out,out* and *in,out* diastereomers were generated but were easily separated, and only the *out,out* form is depicted in Scheme 7. Subsequent reductions afforded the diphosphines **16**, which like **14c** showed significant oxygen sensitivity. Hence, they were characterized *in situ*.

Bauer and Habicher also reported several related triarylphos*phite* and triarylphos*phate* species.[11] In all of their systems, homeomorphic isomerization appeared to be fast on the NMR time scale (e.g., one ^{31}P NMR signal for *in,out* isomers or the presumed *in,in/out,out* mixtures). Dibridgehead di(triaryl)-phosphine dioxides have also been accessed by 3-fold oxidative couplings of the ethynyl-substituted phosphine oxide $OP(p\text{-}C_6H_4OCH_2C{\equiv}CH)_3$ (21% yield, two isomers).[37] All of these approaches to dibridgehead di(triaryl)phosphorus species feature one or more steps with rather low yields, and ours has the added disadvantage of being stoichiometric in a precious metal. However, on the basis of recent work, there is some hope that high-yield sequences might be possible with iron.[38]

Scheme 7. Some Literature Synthesis of Dibridgehead Di(triaryl)phosphine Compounds

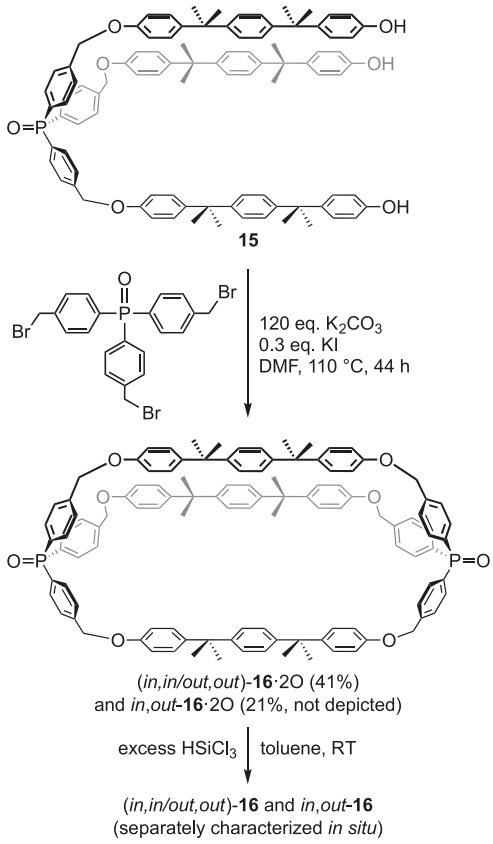

Summary. We have demonstrated that it is possible to synthesize "giant" gyroscope-like molecules that feature dipolar Cl−Rh−CO or $X{-}Re(CO)_3$ rotators and dibridgehead di-(triaryl)phosphine stators via metal-templated 3-fold olefin metatheses. The rotators rapidly rotate within the three 25−29-membered macrocycles in solution. The "rigid" *p*-phenylene units in the stators improve both horizontal and vertical clearance with respect to dibridgehead di(trialkyl)diphosphine

https://doi.org/10.1021/acs.inorgchem.2c02855
Inorg. Chem. 2022, 61, 17012−17025

analogues. However, when the radius of the rotator is increased, such as in p-$CH_3C_6H_4C{\equiv}C{-}Rh{-}CO$, 360° rotation can be blocked. All of these assemblies are structurally porous, but neighboring molecules do not intercalate into the macrocycles. They can, however, occupy the interstices between macrocycles, blocking Cl−Rh−CO rotation in the solid state. This study has also established the feasibility of preparing free dibridgehead di(triaryl)phosphines from the rhodium adducts, a rare class of compounds with unusual stereochemical properties. Future efforts will focus on the further physical and chemical characterization of these metal-free species, as well as syntheses that are not stoichiometric in precious metals.

■ EXPERIMENTAL SECTION

General Data. All reactions were conducted under N_2 or H_2 atmospheres and worked up aerobically. Solvents and reagents were treated as described in the SI, and instrumentation was detailed in a previous paper in the series.[8] NMR spectra are referenced as follows (δ/ppm): ^{1}H, residual internal $CHCl_3$ (7.23), C_6D_5H (7.15), $CHDCl_2$ (5.32), C_6D_4HCl (7.14), $CHFCl_2$ (7.47), $C_6D_5CD_2H$ (2.09); ^{13}C, internal $CDCl_3$ (77.16), C_6D_6 (128.06), CD_2Cl_2 (53.84), C_6D_5Cl (134.19), $CDFCl_2$ (104.2), $C_6D_5CD_3$ (20.4); ^{31}P, internal (capillary) or external H_3PO_4 (0.00).

***trans*-Rh(CO)(Cl)[P(*p*-$C_6H_4O(CH_2)_4CH{=}CH_2)_3$]$_2$ (4a).** A Schlenk flask was charged with **3a** (1.141 g, 2.049 mmol; see the SI), CH_2Cl_2 (30 mL), hexane (30 mL), and [Rh(COD)(μ-Cl)]$_2$ (0.247 g, 0.501 mmol) and flushed with CO. The orange solution was stirred and turned deep yellow. After 2 h, the solvent was removed by an oil pump vacuum. The tan oil was chromatographed on silica gel (2.5 × 7.0 cm column) with hexane/CH_2Cl_2 (1:2, v/v). The solvent was removed from the product fractions by an oil pump vacuum to give **4a** as a yellow solid (1.077 g, 0.8336 mmol, 83%). Anal. Calcd for $C_{73}H_{90}ClO_7P_2Rh$ (1291.92): C, 68.51; H, 7.09. Found: C, 68.11; H, 7.09.

NMR ($CDCl_3$, δ/ppm): ^{1}H 7.62−7.60 (m, 12H, $C_6\underline{H}_4$ *o* to P), 6.88 (d, $^3J_{HH}$ = 7.4 Hz, 12H, $C_6\underline{H}_4$ *m* to P), 5.89−5.83 (m, 6H, C$\underline{H}$=), 5.10−5.00 (m, 12H, =C$\underline{H}_2$), 3.97 (t, $^3J_{HH}$ = 6.5 Hz, 12H, OC$\underline{H}_2$), 2.19−2.14 (m, 12H, C$\underline{H}_2$CH=), 1.85−1.80 (m, 12H, $OCH_2C\underline{H}_2$), 1.65−1.59 (m, 12H, $OCH_2CH_2C\underline{H}_2$); $^{13}C\{^1H\}$[39] 187.7 (dt, $^1J_{RhC}$ = 75.6 Hz, $^2J_{PC}$ = 16.0 Hz, $\underline{C}$O), 160.8 (s, $\underline{C}_6H_4$ *p* to P), 138.9 (s, $\underline{C}$H=), 136.5 (virtual t,[16] $^2J_{PC}$ = 7.0 Hz, $\underline{C}_6H_4$ *o* to P), 125.2 (virtual t,[16] $^1J_{PC}$ = 24.8 Hz, $\underline{C}_6H_4$ *i* to P), 115.2 (s, =$\underline{C}H_2$), 114.5 (virtual t,[16] $^3J_{PC}$ = 5.2 Hz, $\underline{C}_6H_4$ *m* to P), 68.1 (s, O$\underline{C}H_2$), 33.8 (s, $\underline{C}H_2$CH=), 29.1 (s, $OCH_2\underline{C}H_2$), 25.8 (s, $\underline{C}H_2$); $^{31}P\{^1H\}$ 26.0 (d, $^1J_{RhP}$ = 124.6 Hz). IR (cm^{-1}, powder film): 2941 (m), 1972 (s, ν_{CO}), 1594 (s), 1567 (m), 1499 (s), 1474 (m), 1395 (m), 1281 (s), 1246 (s), 1179 (s), 1102 (s).

***trans*-Rh(CO)(Cl)[P(*p*-$C_6H_4O(CH_2)_5CH{=}CH_2)_3$]$_2$ (4b).** **3b** (0.982 g, 1.64 mmol; see the SI), CH_2Cl_2 (30 mL), hexane (30 mL), [Rh(COD)(μ-Cl)]$_2$ (0.197 g, 0.400 mmol), and CO were combined in a procedure analogous to that of **4a**. An identical workup gave **4b** as a yellow solid (0.931 g, 0.683 mmol, 85%). Anal. Calcd for $C_{79}H_{102}ClO_7P_2Rh$ (1363.98): C, 69.57; H, 7.57. Found: C, 68.51; H, 7.72.[40]

NMR ($CDCl_3$, δ/ppm): ^{1}H 7.63−7.61 (m, 12H, $C_6\underline{H}_4$ *o* to P), 6.87 (d, $^3J_{HH}$ = 8.5 Hz, 12H, $C_6\underline{H}_4$ *m* to P), 5.86−5.78 (m, 6H, C$\underline{H}$=), 5.04−4.94 (m, 12H, =C$\underline{H}_2$), 3.95 (t, $^3J_{HH}$ = 6.4 Hz, 12H, OC$\underline{H}_2$), 2.10−2.07 (m, 12H, C$\underline{H}_2$CH=), 1.79−1.77 (m, 12H, $OCH_2C\underline{H}_2$), 1.47−1.45 (m, 24H, $OCH_2CH_2C\underline{H}_2C\underline{H}_2$); $^{13}C\{^1H\}$[39,41] 160.8 (s, $\underline{C}_6H_4$ *p* to P), 139.1 (s, $\underline{C}$H=), 136.5 (virtual t,[16] $^2J_{PC}$ = 7.0 Hz, $\underline{C}_6H_4$ *o* to P), 125.2 (virtual t,[16] $^1J_{PC}$ = 24.8 Hz, $\underline{C}_6H_4$ *i* to P), 114.9 (s, =$\underline{C}H_2$), 114.5 (virtual t,[16] $^3J_{PC}$ = 5.4 Hz, $\underline{C}_6H_4$ *m* to P), 67.2 (s, O$\underline{C}H_2$), 34.1 (s, $\underline{C}H_2$CH=), 29.5 (s, $OCH_2\underline{C}H_2$), 29.0 (s, $\underline{C}H_2$), 26.0 (s, $\underline{C}H_2$); $^{31}P\{^1H\}$ 26.0 (d, $^1J_{RhP}$ = 124.4 Hz). IR (cm^{-1}, powder film): 3076 (w), 2927 (m), 2858 (m), 1966 (s, ν_{CO}), 1640 (m), 1594 (s), 1567 (s), 1497 (s), 1472 (s), 1285 (s), 1246 (s), 1175 (s), 1098 (s).

***trans*-Rh(CO)(Cl)[P(*p*-$C_6H_4O(CH_2)_6CH{=}CH_2)_3$]$_2$ (4c).** **3c** (1.314 g, 2.050 mmol; see the SI), CH_2Cl_2 (30 mL), hexane (30 mL), [Rh(COD)(μ-Cl)]$_2$ (0.246 g, 0.500 mmol), and CO were combined in a procedure analogous to that of **4a**. An identical workup gave **4c** as a yellow solid (1.33 g, 0.918 mmol, 91%). Anal. Calcd for $C_{85}H_{114}ClO_7P_2Rh$ (1448.14): C, 70.57; H, 7.93. Found: C, 68.98; H, 7.81.[40]

NMR ($CDCl_3/C_6D_6$, δ/ppm): ^{1}H 7.62−7.58/8.10−8.06 (m, 12H, $C_6\underline{H}_4$ *o* to P), 6.85/6.84 (d, $^3J_{HH}$ = 10.0/8.7 Hz, 12H, $C_6\underline{H}_4$ *m* to P), 5.85−5.77/5.80−5.72 (m, 6H, C$\underline{H}$=), 5.02−4.92/5.06−4.97 (m, 12H, =C$\underline{H}_2$), 3.95/3.54 (t, $^3J_{HH}$ = 7.5/6.4 Hz, 12H, OC$\underline{H}_2$), 2.08−2.04/1.97−1.92 (m, 12H, C$\underline{H}_2$CH=), 1.80−1.74/1.52−1.48 (m, 12H, $OCH_2C\underline{H}_2$), 1.48−1.41/1.28−1.17 (m, 24H, C$\underline{H}_2$), 1.41−1.34/1.15−1.11 (m, 12H, C$\underline{H}_2$); $^{13}C\{^1H\}$[39] −/188.8 (dt, $^1J_{RhC}$ = 75.0 Hz, $^2J_{PC}$ = 15.5 Hz, $\underline{C}$O), 160.5/161.2 (s, $\underline{C}_6H_4$ *p* to P), 139.2/139.3 (s, $\underline{C}$H=), 136.2/137.0 (virtual t,[16] $^2J_{PC}$ = 6.9/7.0 Hz, $\underline{C}_6H_4$ *o* to P), 124.8/126.0 (virtual t,[16] $^1J_{PC}$ = 25.8/24.7 Hz, $\underline{C}_6H_4$ *i* to P), 114.2/114.8 (virtual t,[16] $^3J_{PC}$ = 5.0/5.4 Hz, $\underline{C}_6H_4$ *m* to P), 114.4/114.7 (s, =$\underline{C}H_2$), 68.0/68.0 (s, O$\underline{C}H_2$), 33.9/34.2 (s, $\underline{C}H_2$CH=), 29.3/29.6 (s, $\underline{C}H_2$), 28.96/29.3 (s, $\underline{C}H_2$), 28.47/29.2 (s, $\underline{C}H_2$), 26.0/26.3 (s, $\underline{C}H_2$); $^{31}P\{^1H\}$ 24.4/26.7 (d, $^1J_{RhP}$ = 123.5/124.4 Hz). IR (cm^{-1}, powder film): 3078 (w), 2929 (m), 2858 (m), 1960 (s, ν_{CO}), 1642 (m), 1594 (s), 1567 (m), 1499 (s), 1470 (m), 1281 (m), 1248 (s), 1179 (s), 1100 (s), 909 (s), 826 (s).

***trans*-Rh(CO)(Cl)[P(*p*-$C_6H_4O(CH_2)_7CH{=}CH_2)_3$]$_2$ (4d).** **3d** (3.608 g, 5.289 mmol; see the SI), CH_2Cl_2 (30 mL), hexane (30 mL), [Rh(COD)(μ-Cl)]$_2$ (0.636 g, 1.29 mmol), and CO were combined in a procedure analogous to that of **4a**. An identical workup gave **4d** as a yellow solid (1.930 g, 1.261 mmol, 49%). Anal. Calcd for $C_{91}H_{126}ClO_7P_2Rh$ (1532.31): C, 71.33; H, 8.29. Found: C, 71.55; H, 8.45.

NMR ($CDCl_3$, δ/ppm): ^{1}H 7.63−7.59 (m, 12H, $C_6\underline{H}_4$ *o* to P), 6.87 (d, $^3J_{HH}$ = 10 Hz, 12H, $C_6\underline{H}_4$ *m* to P), 5.86−5.78 (m, 6H, C$\underline{H}$=), 5.04−4.90 (m, 12H, =C$\underline{H}_2$), 3.95 (t, $^3J_{HH}$ = 5 Hz, 12H, OC$\underline{H}_2$), 2.07−2.03 (m, 12H, C$\underline{H}_2$CH=), 1.80−1.74 (m, 12H, $OCH_2C\underline{H}_2$), 1.46−1.31 (m, 48H, C$\underline{H}_2$); $^{13}C\{^1H\}$ 187.4 (dt, $^1J_{RhC}$ = 75.4 Hz, $^2J_{PC}$ = 16.9 Hz, $\underline{C}$O), 160.5 (s, $\underline{C}_6H_4$ *p* to P), 139.3 (s, $\underline{C}$H=), 136.2 (virtual t,[16] $^2J_{PC}$ = 7.0 Hz, $\underline{C}_6H_4$ *o* to P), 124.8 (virtual t,[16] $^1J_{PC}$ = 28.9 Hz, $\underline{C}_6H_4$ *i* to P), 114.3 (s, =$\underline{C}H_2$), 114.2 (virtual t,[16] $^3J_{PC}$ = 5.7 Hz, $\underline{C}_6H_4$ *m* to P), 68.0 (s, O$\underline{C}H_2$), 33.9 (s, $\underline{C}H_2$CH=), 29.35 (s, $\underline{C}H_2$), 29.32 (s, $\underline{C}H_2$), 29.2 (s, $\underline{C}H_2$), 29.0 (s, $\underline{C}H_2$), 26.1 (s, $\underline{C}H_2$); $^{31}P\{^1H\}$ 25.3 (d, $^1J_{RhP}$ = 125.5 Hz). IR (cm^{-1}, powder film): 2924 (m), 2854 (m), 1965 (s, ν_{CO}), 1642 (m), 1593 (s), 1568 (m), 1497 (s), 1472 (m), 1284 (m), 1246 (s), 1174 (s), 1097 (s), 907 (s), 829 (s).

***trans*-Rh(CO)(Cl)[P(*p*-$C_6H_4O(CH_2)_5CH{=}CH(CH_2)_5O$-*p*-$C_6H_4)_3$P] (5b).** A Schlenk flask was charged with **4b** (0.860 g, 0.630 mmol), Grubbs' first-generation catalyst (ca. half of 0.078 g, 0.094 mmol, 15 mol %), and CH_2Cl_2 (630 mL, giving a 0.0010 M **4b** solution) and fitted with a condenser. The solution was stirred, and the remaining catalyst was added after 24 h. The solution was refluxed, and aliquots were periodically assayed by ^{1}H and $^{31}P\{^1H\}$ NMR. After 48 h, the CH=CH_2 signals had disappeared. The solvent was removed by an oil pump vacuum. The residue was chromatographed on silica gel (2.5 × 10 cm column) using hexane/CH_2Cl_2 (1:3, v/v). The fractions were monitored by thin-layer chromatography. The solvent was removed from those containing only **5b** [R_f = 0.20; 1:3 (v/v) hexane/CH_2Cl_2; a faster eluting material must be separated] by an oil pump vacuum. This gave **5b** as a mixture of C=C isomers and a pale-yellow solid (0.365 g, 0.285 mmol, 45%). Anal. Calcd for $C_{73}H_{90}ClO_7P_2Rh$ (1279.82): C, 68.51; H, 7.09. Found: C, 67.78; H, 7.35.[40]

NMR ($CDCl_3$, δ/ppm, *E*/*Z* mixture): $^{31}P\{^1H\}$ 26.3 (d, $^1J_{RhP}$ = 124.4 Hz, 60%), 26.18 (d, $^1J_{RhP}$ = 124.4 Hz, 30%), 26.06 (d, $^1J_{RhP}$ = 124.4 Hz, 10%). IR (cm^{-1}, powder film): 2925 (m), 2856 (m), 1976 (s, ν_{CO}), 1727 (w), 1594 (s), 1567 (m), 1499 (s), 1468 (m), 1285 (s), 1248 (s), 1179 (s), 1100 (s).

***trans*-Rh(CO)(Cl)[P(*p*-$C_6H_4O(CH_2)_6CH{=}CH(CH_2)_6O$-*p*-$C_6H_4)_3$P] (5c).** **4c** (1.100 g, 0.760 mmol), Grubbs' first-generation catalyst (0.093 g, 0.14 mmol, 15 mol %), and CH_2Cl_2 (760 mL, giving a 0.0010 M **4c** solution) were combined in a procedure analogous to that of **5b**. An identical workup [R_f(**5c**) = 0.30; 1:3 (v/v) hexane/CH_2Cl_2] gave **5c** as a mixture of C=C isomers and a pale-yellow solid (0.506 g, 0.371 mmol, 49%).

https://doi.org/10.1021/acs.inorgchem.2c02855
Inorg. Chem. 2022, 61, 17012−17025

NMR (C_6D_6, δ/ppm, E/Z mixture): $^{31}P\{^1H\}$ 26.3 (d, $^1J_{RhP}$ = 125.7 Hz, 20%), 26.29 (d, $^1J_{RhP}$ = 125.7 Hz, 50%), 20.3 (d, $^1J_{RhP}$ = 125.7 Hz, 30%).

***trans*-Rh(CO)(Cl)[P(*p*-$C_6H_4O(CH_2)_{12}O$-*p*-$C_6H_4)_3P$] (6b).** A Fischer–Porter bottle was charged with **5b** (0.200 g, 0.156 mmol), PtO_2 (0.0071 g, 0.031 mmol, 15 mol %), THF (10 mL), and H_2 (60 psig) with stirring. After 12 h, the solvent was removed by an oil pump vacuum. The residue was filtered through silica gel (2.5 × 5.0 cm) with hexane/CH_2Cl_2 (1:3, v/v). The solvent was removed from the filtrate by an oil pump vacuum to give **6b** as a pale-yellow powder (0.182 g, 0.142 mmol, 91%). Anal. Calcd for $C_{73}H_{96}ClO_7P_2Rh$ (1285.87): C, 68.19; H, 7.53. Found: C, 67.83; H, 8.05.

NMR ($CDCl_3$, δ/ppm): ^1H 7.73–7.67 (m, 12H, $C_6\underline{H}_4$ *o* to P), 6.92 (d, $^3J_{HH}$ = 8.5 Hz, 12H, $C_6\underline{H}_4$ *m* to P), 4.06 (t, $^3J_{HH}$ = 6.6 Hz, 12H, $OC\underline{H}_2$), 1.82–1.77 (m, 12H, $OCH_2C\underline{H}_2$), 1.47–1.44 (m, 12H, $OCH_2CH_2C\underline{H}_2$), 1.33–1.30 (m, 36H, $OCH_2CH_2CH_2C\underline{H}_2C\underline{H}_2C\underline{H}_2$); $^{13}C\{^1H\}$[39] 187.8 (dt, $^1J_{RhC}$ = 74.7 Hz, $^2J_{PC}$ = 15.6 Hz, $\underline{C}O$), 160.7 (s, $\underline{C}_6H_4$ *p* to P), 136.5 (virtual t,[16] $^2J_{PC}$ = 7.1 Hz, $\underline{C}_6H_4$ *o* to P), 124.7 (virtual t,[16] $^1J_{PC}$ = 25.0 Hz, $\underline{C}_6H_4$ *i* to P), 114.9 (virtual t,[16] $^3J_{PC}$ = 5.5 Hz, $\underline{C}_6H_4$ *m* to P), 68.1 (s, $O\underline{C}H_2$), 29.9 (s, $OCH_2\underline{C}H_2$), 29.5 (s, $\underline{C}H_2$), 29.1 (s, $\underline{C}H_2$), 28.9 (s, $\underline{C}H_2$), 26.1 (s, $\underline{C}H_2$); $^{31}P\{^1H\}$ 25.9 (d, $^1J_{RhP}$ = 124.0 Hz). IR (cm^{-1}, powder film): 2925 (m), 2962 (w), 2923 (w), 2852 (w), 1976 (s, ν_{CO}), 1727 (w), 1594 (s), 1567 (m), 1497 (s), 1468 (m), 1287 (s), 1248 (s), 1179 (s), 1100 (s).

***trans*-Rh(CO)(Cl)[P(*p*-$C_6H_4O(CH_2)_{14}O$-*p*-$C_6H_4)_3P$] (6c).** **5c** (0.506 g, 0.371 mmol), PtO_2 (0.0127 g, 0.0559 mmol), THF (20 mL), and H_2 (60 psig) were combined in a procedure analogous to that of **6b**. An identical workup gave crude **6c** as a yellow powder (0.442 g, 0.322 mmol, 87%; ca. 90% purity by ^{31}P NMR), which was crystallized from THF/methanol to give **6c** (0.270 g, 0.197 mmol, 53%; >98% purity). Anal. Calcd for $C_{79}H_{108}ClO_7P_2Rh$ (1370.03): C, 69.26; H, 8.17. Found: C, 68.04; H, 7.94.[40]

NMR ($CDCl_3/C_6D_6$, δ/ppm): ^1H 7.67–7.63/8.10–8.03 (m, 12H, $C_6\underline{H}_4$ *o* to P), 6.90/6.79 (d, $^3J_{HH}$ = 8.8/8.5 Hz, 12H, $C_6\underline{H}_4$ *m* to P), 3.99/3.59 (t, $^3J_{HH}$ = 6.9/6.6 Hz, 12H, $OC\underline{H}_2$), 1.77/1.60–1.53 (m, 12H, $OCH_2C\underline{H}_2$), 1.47–1.25/1.34–1.20 (m, 60H, $OCH_2CH_2C\underline{H}_2C\underline{H}_2C\underline{H}_2C\underline{H}_2C\underline{H}_2$); $^{13}C\{^1H\}$[39] −/188.5 (dt, $^1J_{RhC}$ = 75.2 Hz, $^2J_{PC}$ = 15.4 Hz, $\underline{C}O$), 160.5/161.2 (s, $\underline{C}_6H_4$ *p* to P), 136.2/137.6 (virtual t,[16] $^2J_{PC}$ = 6.7/6.9 Hz, $\underline{C}_6H_4$ *o* to P), −/126.0 (virtual t,[16] $^1J_{PC}$ = 25.0 Hz, $\underline{C}_6H_4$ *i* to P), 114.4/114.9 (virtual t,[16] $^3J_{PC}$ = 5.4/5.5 Hz, $\underline{C}_6H_4$ *m* to P), 67.7/67.9 (s, $O\underline{C}H_2$), 29.7/30.1 (s, $\underline{C}H_2$), 29.5/29.9 (s, $\underline{C}H_2$), 29.3/29.5 (s, $\underline{C}H_2$), 28.94/29.4 (s, $\underline{C}H_2$), 28.88/29.3 (s, $\underline{C}H_2$), 25.8/26.3 (s, $\underline{C}H_2$); $^{31}P\{^1H\}$ 25.5/26.1 (d, $^1J_{RhP}$ = 123.5/125.4 Hz). IR (cm^{-1}, powder film): 2923 (s), 2854 (m), 1972 (s, ν_{CO}), 1594 (s), 1567 (m), 1497 (s), 1468 (m), 1285 (s), 1248 (s), 1177 (s), 1098 (s), 1023 (m), 824 (s).

***trans*-Rh(CO)(Cl)[P(*p*-$C_6H_4O(CH_2)_{16}O$-*p*-$C_6H_4)_3P$] (6d).** A round-bottom flask was charged with **5d** (1.462 g, 0.9551 mmol) and CH_2Cl_2 (950 mL, giving a ∼0.001 M **5d** solution) and fitted with a condenser. A solution of Grubbs' first-generation catalyst (0.059 g, 0.072 mmol, 7.5 mol %) in CH_2Cl_2 (10 mL) was added via a syringe. The mixture was stirred for 24 h. A second equal charge of Grubbs' catalyst was added, and the mixture was kept at 40 °C. After 48 h (reaction incomplete by ^1H NMR), a third equal charge of Grubbs' catalyst was added. After 48 h (reaction complete), the mixture was allowed to cool and filtered through neutral alumina (5.0 × 60.0 cm column), which was washed with additional CH_2Cl_2 (1000 mL). The solvent was removed from the filtrate/washings by rotary evaporation. The dark-yellow oil was dissolved in THF (20 mL) and transferred to a Fisher-Porter bottle that had been charged with PtO_2 (0.033 g, 0.14 mmol, 15 mol %). The mixture was stirred under H_2 (75 psig). After 12 h, the solvent was removed by rotary evaporation. The black residue was chromatographed on silica (5.0 × 30.0 cm column) using a 1:1 (v/v) hexane/CH_2Cl_2. The solvent was removed from the product fractions to give **6d** as a yellow solid (0.366 g, 0.252 mmol, 26%), which decomposed without melting between 105 and 120 °C. Anal. Calcd for $C_{85}H_{120}ClO_7P_2Rh$ (1452.73): C, 70.21; H, 8.32, Found: C, 69.59; H, 8.38.[40]

NMR ($CDCl_3$, δ/ppm): ^1H (500 MHz) 7.64 (virtual dt,[16] $^3J_{HH}$ = 8.8 Hz, $^3J_{PH}$ = 5.2 Hz, 12H, $C_6\underline{H}_4$ *o* to P), 6.89 (d, $^3J_{HH}$ = 8.8 Hz, 12H, $C_6\underline{H}_4$ *m* to P), 3.97 (t, $^3J_{HH}$ = 6.4 Hz, 12H, $OC\underline{H}_2$), 1.80–1.75 (m, 14H, $C\underline{H}_2$), 1.49–1.43 (m, 14H, $C\underline{H}_2$), 1.35–1.27 (m, 56H, $C\underline{H}_2$); $^{13}C\{^1H\}$ (126 MHz) 187.4 (dt, $^1J_{RhC}$ = 73.2 Hz, J_{PC} = 16.4 Hz, $\underline{C}O$), 160.6 (s, $\underline{C}_6H_4$ *p* to P), 136.2 (virtual t,[16] $^2J_{PC}$ = 7.1 Hz, $\underline{C}_6H_4$ *o* to P), 124.7 (virtual t,[16] $^1J_{PC}$ = 24.8 Hz, $\underline{C}_6H_4$ *i* to P), 114.3 (virtual t,[16] $^3J_{PC}$ = 5.5 Hz, $\underline{C}_6H_4$ *m* to P), 67.8 (s, $O\underline{C}H_2$), 29.57 (s, $OCH_2\underline{C}H_2$), 29.54 (s, $\underline{C}H_2$), 29.2 (s, $\underline{C}H_2$), 29.1 (s, $\underline{C}H_2$), 29.08 (s, $\underline{C}H_2$), 29.06 (s, $\underline{C}H_2$); $^{31}P\{^1H\}$ 25.2 (d, $^1J_{RhP}$ = 125.2 Hz). IR (cm^{-1}, powder film): 2922 (m), 2850 (m), 1971 (s, ν_{CO}), 1593 (m), 1497 (m).

***trans*-Rh(CO)(C≡CC_6H_5)[P(*p*-$C_6H_4O(CH_2)_{12}O$-*p*-$C_6H_4)_3P$] (7b).** A Schlenk tube was charged with HC≡CC_6H_5 (1.0 M in hexane; 0.080 mL, 0.080 mmol) and THF (2 mL) and cooled to −78 °C. Then *n*-BuLi (2.5 M in hexane; 0.040 mL, 0.10 mmol) was added with stirring. After 1.5 h, a solution of **6b** (0.052 g, 0.040 mmol) in THF (2 mL) was added by cannula. The cold bath was kept at −78 °C for 1 h and then allowed to warm to room temperature. After 3 h, the solvent was removed by an oil pump vacuum. The residue was washed with hexane (2 × 2 mL) and chromatographed on neutral alumina (2.5 × 7.0 cm column) with hexane/THF (1:1, v/v). The solvent was removed from the yellow fraction by an oil pump vacuum to give **7b** as a dark-yellow powder (0.012 g, 0.0089 mmol, 22%). Anal. Calcd for $C_{81}H_{101}O_7P_2Rh$ (1351.55): C, 71.98; H, 7.53. Found: C, 70.23; H, 8.16.[40]

NMR (CD_2Cl_2, δ/ppm): ^1H 7.73–7.69 (m, 12H, $C_6\underline{H}_4$ *o* to P), 6.92–6.84 (m, 12H + 3H, $C_6\underline{H}_4$ *m* to P + 3H of C≡$CC_6\underline{H}_5$), 6.51–6.47 (m, 2H of C≡$CC_6\underline{H}_5$), 4.02 (t, $^3J_{HH}$ = 6.7 Hz, 12H, $OC\underline{H}_2$), 1.81–1.70 (m, 12H, $OCH_2C\underline{H}_2$), 1.54–1.20 (m, 48H, $OCH_2CH_2C\underline{H}_2C\underline{H}_2C\underline{H}_2C\underline{H}_2$); $^{13}C\{^1H\}$[39] 193.2 (dt, $^1J_{RhC}$ = 59.6 Hz, $^2J_{PC}$ = 14.0 Hz, $\underline{C}O$), 160.6 (s, $\underline{C}_6H_4$ *p* to P), 136.3 (virtual t,[16] $^2J_{PC}$ = 7.1 Hz, $\underline{C}_6H_4$ *o* to P), 130.7 (s, C≡$C\underline{C}_6H_5$), 128.5 (s, C≡$C\underline{C}_6H_5$), 127.7 (s, C≡$C\underline{C}_6H_5$), 126.6 (virtual t,[16] $^1J_{PC}$ = 24.6 Hz, $\underline{C}_6H_4$ *i* to P), 124.6 (s, C≡$C\underline{C}_6H_5$), 121.5–121.3 (apparent m, $\underline{C}$≡$\underline{C}$),[42] 114.6 (virtual t,[16] $^3J_{PC}$ = 5.5 Hz, $\underline{C}_6H_4$ *m* to P), 68.2 (s, $O\underline{C}H_2$), 29.8 (s, $OCH_2\underline{C}H_2$), 29.4 (s, $\underline{C}H_2$), 29.0 (s, $\underline{C}H_2$), 28.9 (s, $\underline{C}H_2$), 26.0 (s, $\underline{C}H_2$); $^{31}P\{^1H\}$ 29.7 (d, $^1J_{RhP}$ = 133.0 Hz). IR (cm^{-1}, powder film): 3061 (w), 2926 (s), 2856 (s), 2339 (w, $\nu_{C\equiv C}$), 1976 (s, ν_{CO}), 1594 (s), 1567 (m), 1497 (s), 1467 (m), 1251 (s), 1177 (s), 1100 (s), 1023 (s).

***trans*-Rh(CO)(C≡CC_6H_4-*p*-CH_3)[P(*p*-$C_6H_4O(CH_2)_{12}O$-*p*-$C_6H_4)_3P$] (8b).** HC≡CC_6H_4-*p*-CH_3 (0.50 M in THF; 0.200 mL, 0.10 mmol), THF (2 mL), *n*-BuLi (2.5 M in hexane; 0.048 mL, 0.12 mmol), and **6b** (0.084 g, 0.080 mmol) in THF (2 mL) were combined in a procedure analogous to that of **7b**. An identical workup gave **8b** as a dark-yellow powder (0.040 g, 0.029 mmol, 37%). Anal. Calcd for $C_{82}H_{103}O_7P_2Rh$ (1365.57): C, 72.12; H, 7.60. Found: C, 72.85; H, 8.41.[40]

NMR (CD_2Cl_2, δ/ppm): ^1H 7.92–7.87 (m, 8H, $C_6\underline{H}_4$ *o* to P), 7.35–7.32 (m, 4H, $C_6\underline{H}_4$ *o* to P), 6.93 (d, $^3J_{HH}$ = 8.4 Hz, 8H, $C_6\underline{H}_4$ *m* to P), 6.85 (d, $^3J_{HH}$ = 8.4 Hz, 4H, $C_6\underline{H}_4$ *m* to P), 6.74 (d, $^3J_{HH}$ = 7.8 Hz, 2H, C≡$CC_6\underline{H}_4$), 6.36 (d, $^3J_{HH}$ = 7.8 Hz, 2H, C≡$CC_6\underline{H}_4$), 4.06–4.00 (m, 12H, $OC\underline{H}_2$), 2.17 (s, 3H, $C\underline{H}_3$), 1.76–1.69 (m, 12H, $OCH_2C\underline{H}_2$), 1.40–1.21 (m, 48H, $OCH_2CH_2C\underline{H}_2C\underline{H}_2C\underline{H}_2C\underline{H}_2$); $^{13}C\{^1H\}$[39] 193.1 (d,[43] $^1J_{RhC}$ = 59.2 Hz, $\underline{C}O$), 160.8 (s, $\underline{C}_6H_4$ *p* to P),[44] 160.2 (s, $\underline{C}_6H_4$ *p* to P), 137.3 (virtual t,[16] $^2J_{PC}$ = 7.4 Hz, $\underline{C}_6H_4$ *o* to P),[44] 134.6 (s, C≡$C\underline{C}_6H_4$), 134.4 (virtual t,[16] $^2J_{PC}$ = 7.0 Hz, $\underline{C}_6H_4$ *o* to P), 130.6 (s, C≡$C\underline{C}_6H_4$), 129.3 (virtual t,[16] $^1J_{PC}$ = 23.6 Hz, $\underline{C}_6H_4$ *i* to P), 128.4 (s, C≡$C\underline{C}_6H_4$), 125.5 (s, C≡$C\underline{C}_6H_4$), 125.3 (virtual t,[16] $^1J_{PC}$ = 25.0 Hz, $\underline{C}_6H_4$ *i* to P),[44] 121.6–121.3 (apparent m, $\underline{C}$≡$\underline{C}$),[42] 114.69 (virtual t,[16] $^3J_{PC}$ = 5.6 Hz, $\underline{C}_6H_4$ *m* to P), 114.61 (virtual t,[16] $^3J_{PC}$ = 5.6 Hz, $\underline{C}_6H_4$ *m* to P),[44] 68.2 (s, $O\underline{C}H_2$),[44] 68.0 (s, $O\underline{C}H_2$), 29.82 (s, $\underline{C}H_2$), 29.78 (s, $\underline{C}H_2$),[44] 29.6 (s, $\underline{C}H_2$), 29.4 (s, $\underline{C}H_2$),[44] 29.13 (s, $\underline{C}H_2$), 29.06 (s, $\underline{C}H_2$),[44] 28.91 (s, $\underline{C}H_2$), 28.86 (s, $\underline{C}H_2$),[44] 26.03 (s, $\underline{C}H_2$),[44] 25.95 (s, $\underline{C}H_2$), 21.3 ($\underline{C}H_3$); $^{31}P\{^1H\}$ 29.3 (d, $^1J_{RhP}$ = 133.5 Hz). IR (cm^{-1}, powder film): 3065(s), 2926 (s), 2853 (s), 2339 (w, $\nu_{C\equiv C}$), 1972 (s, ν_{CO}), 1594 (s), 1567 (m), 1498 (s), 1467 (m), 1251 (s), 1177 (s), 1096 (s), 1023 (s).

P(*p*-$C_6H_4O(CH_2)_{14}O$-*p*-$C_6H_4)_3P$ (14c). A scintillation vial was charged with **6c** (0.063 g, 0.046 mmol), hexanes (10 mL), and PMe_3 (1.0 M in toluene, 0.46 mL, 0.46 mmol) with stirring. After 24 h, the solution was passed through a pipet of silica, which was rinsed with

https://doi.org/10.1021/acs.inorgchem.2c02855
Inorg. Chem. 2022, 61, 17012−17025

CH_2Cl_2 (20 mL). The solvent was removed from the filtrate by an oil pump vacuum to give **14c** (0.046 g, 0.038 mmol, 83%) as a white solid with a melting point of 123−128 °C. Then THF (20 mL) was added to the silica gel to extract the yellow residue. The solvent was removed from the extract by an oil pump vacuum to give a mixture of **6d**, *trans*-$Rh(CO)(Cl)(PMe_3)_2$,[29] and other species. Anal. Calcd for $C_{78}H_{108}O_6P_2$ (1202.76): C, 77.83; H, 9.04. Found: C, 77.10; H, 9.00.

NMR (toluene-d_8, δ/ppm): ^{1}H (500 MHz) 7.37 (dd, $^3J_{PH}$ = 6.9 Hz, $^3J_{HH}$ = 8.6 Hz, 12H, *o*-$C_6\underline{H}_4$), 6.77 (apparent d, $^3J_{HH}$ = 8.3 Hz, 12H, *m*-$C_6\underline{H}_4$), 3.61 (t, $^3J_{HH}$ = 6.4 Hz, 12H, $OC\underline{H}_2$), 1.62−1.57 (m, 12H, $C\underline{H}_2$), 1.38−1.33 (m, 12H, $C\underline{H}_2$), 1.30−1.23 (m, 48H, $C\underline{H}_2$); ^{13}C {^{1}H} (126 MHz) 160.2 (s, $\underline{C}_6H_4$ *p* to P), 135.6−135.3 (br d, $\underline{C}_6H_4$ *i* to P), 130.0 (d, J_{PC} = 9.9 Hz, $\underline{C}_6H_4$), 115.0 (d, J_{PC} = 7.4 Hz, $\underline{C}_6H_4$), 67.8 (s, $O\underline{C}H_2$), 29.89 (s, $\underline{C}H_2$), 29.88 (s, $\underline{C}H_2$), 29.8 (s, $\underline{C}H_2$), 29.7 (s, $C\underline{H}_2$), 29.6 (s, $\underline{C}H_2$), 26.5 (s, $C\underline{H}_2$); ^{31}P{^{1}H} (202 MHz) −5.2 (s). IR (powder film, cm^{-1}): 2920 (m), 2850 (m), 1591 (m), 1495 (m), 1276 (m), 1242 (s), 1174 (s).

P(*p*-$C_6H_4O(CH_2)_{16}O$-*p*-$C_6H_4)_3P$ (14d). A scintillation vial was charged with **6d** (0.120 g, 0.0826 mmol), hexanes (15 mL), and PMe_3 (1.0 M in toluene, 0.83 mL, 0.83 mmol) with stirring. After 24 h, the yellow slurry was filtered through glass wool. The wool retained a yellow solid, which was rinsed with hexanes (5 mL). The filtrate was filtered through a pipet of silica gel, which was rinsed with hexanes (15 mL) followed by CH_2Cl_2 (5 mL). The solvent was removed from the filtrate by an oil pump vacuum to give **14d** (0.080 g, 0.062 mmol, 75%) as a white solid with a melting point of 138−143 °C. Then CH_2Cl_2 (10 mL) and THF (10 mL) were added to the silica gel to extract the yellow residue. The solvent was removed from the extract by an oil pump vacuum to give a mixture of **6d**, *trans*-$Rh(CO)(Cl)(PMe_3)_2$,[29] and other species. Anal. Calcd for $C_{84}H_{120}O_6P_2$ (1286.86): C, 78.34; H, 9.39. Found: C, 76.81; H, 9.32.[28,40]

NMR (toluene-d_8, δ/ppm): ^{1}H (500 MHz) 7.38 (dd, $^3J_{PH}$ = 7.0 Hz, $^3J_{HH}$ = 8.7 Hz, 12H, *o*-$C_6\underline{H}_4$), 6.77 (dd, $^3J_{HH}$ = 8.7 Hz, $^4J_{PH}$ = 0.7 Hz, 12H, *m*-$C_6\underline{H}_4$), 3.60 (t, $^3J_{HH}$ = 6.5 Hz, 12H, $OC\underline{H}_2$), 1.62−1.56 (m, 12H, $C\underline{H}_2$), 1.37−1.32 (m, 12H, $C\underline{H}_2$), 1.32−1.22 (m, 60H, $C\underline{H}_2$); ^{13}C {^{1}H} (126 MHz) 160.2 (s, $\underline{C}_6H_4$ *p* to P), 135.5−135.3 (br d, $\underline{C}_6H_4$ *i* to P), 130.0 (d, J_{PC} = 10.0 Hz, $\underline{C}_6H_4$), 115.0 (d, J_{PC} = 7.6 Hz, $\underline{C}_6H_4$), 67.8 (s, $O\underline{C}H_2$), 30.0 (2 × overlapping s, $\underline{C}H_2$), 29.95 (s, $\underline{C}H_2$), 29.90 (s, $\underline{C}H_2$), 29.7 (s, $C\underline{H}_2$), 29.6 (s, $\underline{C}H_2$), 26.5 (s, $C\underline{H}_2$); ^{31}P{^{1}H} (202 MHz) −5.1 (s). IR (powder film, cm^{-1}): 2920 (m), 2850 (m), 1593 (m), 1496 (m), 1276 (m), 1242 (s), 1174 (s).

Reactions of 14c and 14d. (A) A scintillation vial was charged with $[Rh(CO)_2(\mu\text{-}Cl)]_2$ (0.006 g, 0.02 mmol) and CH_2Cl_2 (5 mL). A solution of **14d** (0.038 g, 0.030 mmol) in CH_2Cl_2 (5 mL) was added with stirring. After 24 h, the mixture was passed through a pipet of silica, which was rinsed with CH_2Cl_2 (10 mL). The yellow fraction was collected and the solvent removed by an oil pump vacuum to give **6d** as a yellow solid (0.038 g, 0.026 mmol, 87%). (B) A J. Young valve NMR tube was charged with a solution of **14c** (0.015 g, 0.013 mmol) or **14d** (0.015 g, 0.012 mmol) in C_6D_5Br (1.0 mL) and kept at 140 ± 1 °C (oil bath).[28] The tube was periodically removed from the bath, and ^{1}H, ^{13}C{^{1}H}, and ^{31}P{^{1}H} NMR spectra were recorded. Representative data are given in Figure s10.

***mer,trans*-$Re(CO)_3(Cl)[P(p\text{-}C_6H_4O(CH_2)_6CH{=}CH_2)_3]_2$ (10c).** A Schlenk flask was charged with $Re(CO)_5(Cl)$ (0.361 g, 0.998 mmol),[25] chlorobenzene (15 mL), and **3c** (1.501 g, 2.342 mmol) and fitted with a condenser. The yellow solution was stirred at 140 °C (24 h) and became orange as gas evolved. The solution was cooled, and the solvent was removed by rotary evaporation and an oil pump vacuum. The residue was chromatographed (Al_2O_3, 3 × 15 cm column) with hexane/CH_2Cl_2 (first 2:1 and later 1:1, v/v). The solvent was removed from the major yellow band by an oil pump vacuum to give **10c** (0.901 g, 0.568 mmol, 57%) as a viscous yellow oil. Anal. Calcd for $C_{87}H_{114}ClO_9P_2Re$ (1587.46): C, 65.82; H, 7.24. Found: C, 67.59; H, 7.64.[40]

NMR (C_6D_6, δ/ppm): ^{1}H[39] 8.20−8.00 (br m, 12H, $C_6\underline{H}_4$), 6.91−6.72 (br m, 12H, $C_6\underline{H}_4$), 5.88−5.69 (br m, 6H, $C\underline{H}{=}$), 5.13−4.92 (br m, 12H, $={C\underline{H}_2}$), 3.62−2.93 (br m, 12H, $OC\underline{H}_2$), 2.04−1.88 (br m, 12H, $C\underline{H}_2CH{=}CH_2$), 1.61−1.40 (br m, 12H, $OCH_2C\underline{H}_2$), 1.37−1.02 (br m, 36H, $C\underline{H}_2$); ^{13}C{^{1}H}[39] 194.6 (t, $^2J_{PC}$ = 8.7 Hz, $\underline{C}O$ *trans* to CO), 190.7 (t, $^2J_{PC}$ = 5.6 Hz, $\underline{C}O$ *trans* to Cl), 160.9 (s, $\underline{C}_6H_4$ *p* to P), 139.1 (s, $\underline{C}H{=}$), 135.9 (virtual t,[16] $^2J_{PC}$ = 6.0 Hz, $\underline{C}_6H_4$ *o* to P), 127.2 (virtual t,[16] $^1J_{PC}$ = 26.3 Hz, $\underline{C}_6H_4$ *i* to P), 114.7 (virtual t,[16] $^3J_{PC}$ = 5.1 Hz, $\underline{C}_6H_4$ *m* to P), 114.6 (s, $={\underline{C}H_2}$), 67.8 (s, $O\underline{C}H_2$), 34.0 (s, $\underline{C}H_2$), 29.3 (s, $\underline{C}H_2$), 29.1 (s, $\underline{C}H_2$), 29.0 (s, $\underline{C}H_2$), 26.1 (s, $\underline{C}H_2$); ^{31}P{^{1}H} 5.4 (s). IR (cm^{-1}, oil film): 2044 (w, ν_{CO}), 1938 (s, ν_{CO}), 1900 (s, ν_{CO}), 1640 (m, $\nu_{C=C}$).

***mer,trans*-$Re(CO)_3(Br)[P(p\text{-}C_6H_4O(CH_2)_6CH{=}CH_2)_3]_2$ (11c).** $Re(CO)_5(Br)$ (0.500 g, 1.23 mmol),[25] chlorobenzene (20 mL), and **3c** (1.576 g, 2.459 mmol) were combined in a procedure analogous to **10c**. An identical workup gave **11c** (1.381 g, 0.8463 mmol, 69%) as a viscous yellow oil. Anal. Calcd for $C_{87}H_{114}BrO_9P_2Re$ (1631.92): C, 64.03; H, 7.04. Found: C, 65.77; H, 7.24.[40]

NMR (C_6D_6, δ/ppm): ^{1}H[39] 8.19−7.99 (br m, 12H, $C_6\underline{H}_4$), 6.92−6.67 (br m, 12H, $C_6\underline{H}_4$), 5.85−5.69 (br m, 6H, $C\underline{H}{=}$), 5.02 (br d, $^3J_{HH,trans}$ = 18.7 Hz, 6H, $={CH_E\underline{H}_Z}$), 4.99 (br d, $^3J_{HH,cis}$ = 10.2 Hz, 6H, $={C\underline{H}_EH_Z}$), 3.50 (t, 12H, $^3J_{HH}$ = 5.8 Hz, $OC\underline{H}_2$), 2.07−1.88 (br m, 12H, $C\underline{H}_2CH{=}CH_2$), 1.58−1.42 (br m, 12H, $OCH_2C\underline{H}_2$), 1.37−1.06 (br m, 36H, $C\underline{H}_2$); ^{13}C{^{1}H}[39] 193.8 (t, $^2J_{PC}$ = 8.8 Hz, $\underline{C}O$ *trans* to CO), 190.3 (t, $^2J_{PC}$ = 5.7 Hz, $\underline{C}O$ *trans* to Br), 160.9 (s, $\underline{C}_6H_4$ *p* to P), 139.1 (s, $\underline{C}H{=}$), 136.0 (virtual t,[16] $^2J_{PC}$ = 5.9 Hz, C_6H_4 *o* to P), 127.1 (virtual t,[16] $^1J_{PC}$ = 26.4 Hz, $\underline{C}_6H_4$ *i* to P), 114.6 (virtual t,[16] $^3J_{PC}$ = 5.2 Hz, $\underline{C}_6H_4$ *m* to P), 114.5 (s, $={\underline{C}H_2}$), 67.8 (s, $O\underline{C}H_2$), 34.0 (s, $\underline{C}H_2$), 29.3 (s, $\underline{C}H_2$), 29.1 (s, $\underline{C}H_2$), 29.0 (s, $\underline{C}H_2$), 26.1 (s, $\underline{C}H_2$); ^{31}P{^{1}H} 2.7 (s). IR (cm^{-1}, oil film): 2045 (w, ν_{CO}), 1939 (s, ν_{CO}), 1902 (s, ν_{CO}), 1641 (m, $\nu_{C=C}$).

***mer,trans*-$Re(CO)_3(Cl)[P(p\text{-}C_6H_4O(CH_2)_{14}O\text{-}p\text{-}C_6H_4)_3P]$ (12c).** A Schlenk flask was charged with **10c** (0.836 g, 0.527 mmol), chlorobenzene (500 mL, giving a 0.0011 M **10c** solution), and Grubbs' first-generation catalyst (0.022 g, 0.027 mmol, 5 mol %). The mixture was stirred for 1 day, while N_2 was aspirated through the solution to remove ethylene. Aliquots were periodically assayed by ^{1}H NMR (C_6D_6, disappearance of $CH{=}CH_2$, and formation of $CH{=}CH$ signals). The sample was filtered through Al_2O_3, which was rinsed with CH_2Cl_2. The solvent was removed from the combined filtrates by an oil pump vacuum to give the crude metathesis product as a viscous yellow oil (0.820 g); the ^{1}H NMR spectrum showed residual chlorobenzene.

NMR (C_6D_6, δ/ppm, *E*/*Z* mixture): ^{1}H 8.30−7.80 (br m, 12H, $C_6\underline{H}_4$), 6.87−6.67 (br m, 12H, $C_6\underline{H}_4$), 5.58−5.30 (br m, 6H, $C\underline{H}{=}$), 3.80−3.42 (br m, 12H, $OC\underline{H}_2$), 2.18−1.87 (m, 12H, $C\underline{H}_2CH{=}CH$), 1.68−1.46 (m, 12H, $OCH_2C\underline{H}_2$), 1.42−1.02 (m, 36H, $C\underline{H}_2$); ^{31}P{^{1}H} 5.7 (s, 11%), 5.6 (s, 25%), 5.5 (s, 20%), 5.1 (s, 45%).

A Schlenk flask was charged with the crude metathesis product (0.820 g), THF (10 mL), and PtO_2 (0.012 g, 0.053 mmol) and partially evacuated. Then H_2 was introduced and the pressure maintained by a balloon. The suspension was stirred. After 24 h, the solvent was removed by an oil pump vacuum. The residue was chromatographed (Al_2O_3, 3 × 25 cm column) with hexane/CH_2Cl_2 (first 2:1 and later 1:2, v/v). The solvent was removed from the product fractions by rotary evaporation and an oil pump vacuum to give **12c** as a white solid (0.148 g, 0.0980 mmol; 19% from **10c**), which decomposed between 150 °C (onset of darkening) and 215 °C. Anal. Calcd for $C_{81}H_{108}ClO_9P_2Re$ (1509.35): C, 64.46; H, 7.21. Found: C, 64.47; H, 7.10.

NMR (C_6D_6, δ/ppm): ^{1}H 8.31−7.88 (br m, 12H, $C_6\underline{H}_4$), 7.00−6.68 (br m, 12H, $C_6\underline{H}_4$), 3.73−3.45 (br m, 12H, $OC\underline{H}_2$), 1.70−1.50 (m, 12H, $OCH_2C\underline{H}_2$), 1.49−1.01 (m, 60H, $C\underline{H}_2$); ^{13}C{^{1}H} 194.6 (t, $^2J_{PC}$ = 9.0 Hz, $\underline{C}O$ *trans* to CO), 190.5 (t, $^2J_{PC}$ = 5.2 Hz, $\underline{C}O$ *trans* to Cl), 160.9 (s, $\underline{C}_6H_4$ *p* to P), 135.9 (virtual t,[16] $^2J_{PC}$ = 6.1 Hz, $\underline{C}_6H_4$ *o* to P), 126.7 (virtual t,[16] $^1J_{PC}$ = 26.1 Hz, $\underline{C}_6H_4$ *i* to P), 114.7 (virtual t,[16] $^3J_{PC}$ = 5.4 Hz, $\underline{C}_6H_4$ *m* to P), 67.8 (s, $O\underline{C}H_2$), 30.0 (s, $\underline{C}H_2$), 29.7 (s, $\underline{C}H_2$), 29.4 (s, $\underline{C}H_2$), 29.3 (s, $\underline{C}H_2$), 29.1 (s, $\underline{C}H_2$), 26.1 (s, $\underline{C}H_2$); ^{31}P{^{1}H} 5.7 (s). IR (cm^{-1}, powder film): 2039 (m, ν_{CO}), 1938 (s, ν_{CO}), 1902 (s, ν_{CO}).

***mer,trans*-$Re(CO)_3(Br)[P(p\text{-}C_6H_4O(CH_2)_{14}O\text{-}p\text{-}C_6H_4)_3P]$ (13c).** **11c** (1.301 g, 0.7972 mmol), chlorobenzene (700 mL, giving a 0.0011 M **11c** solution), and Grubbs' first-generation catalyst (0.033 g, 0.040 mmol, 5 mol %) were combined in a procedure analogous to that of **12c**. An identical workup gave the crude metathesis product as a viscous yellow oil (0.866 g, 0.592 mmol, 74%).

NMR (C_6D_6, δ/ppm, *E*/*Z* mixture): ^{1}H 8.30−7.61 (br m, 12H, $C_6\underline{H}_4$), 6.95−6.67 (br m, 12H, $C_6\underline{H}_4$), 5.58−5.30 (br m, 6H, $C\underline{H}{=}$), 3.82−3.38 (br m, 12H, $OC\underline{H}_2$), 2.18−1.87 (m, 12H, $C\underline{H}_2CH{=}CH$),

https://doi.org/10.1021/acs.inorgchem.2c02855
Inorg. Chem. 2022, 61, 17012−17025

1.68−1.46 (m, 12H, $OCH_2C\underline{H}_2$), 1.42−1.04 (m, 36H, $C\underline{H}_2$); $^{31}P\{^1H\}$ 3.2 (s, 13%), 3.1 (s, 20%), 3.0 (s, 17%), 2.6 (s, 50%).

The crude metathesis product (0.567 g, 0.387 mmol), THF (20 mL), PtO_2 (0.013 g, 0.057 mmol), and H_2 (75 psig) were combined in a procedure analogous to that of **12c** but using a Fisher-Porter bottle. An identical workup gave **13c** as a white solid (0.464 g, 0.316 mmol; 61% from **11c**), which decomposed between 75 °C (onset of darkening) and 137 °C. Anal. Calcd for $C_{81}H_{108}BrO_9P_2Re$ (1553.80): C, 62.61; H, 7.01. Found: C, 62.22; H, 6.69.

NMR (C_6D_6, δ/ppm): ^1H 8.08−7.92 (br m, 12H, $C_6\underline{H}_4$), 6.88−6.72 (br m, 12H, $C_6\underline{H}_4$), 3.71−3.50 (br m, 12H, $OC\underline{H}_2$), 1.68−1.48 (m, 12H, $OCH_2C\underline{H}_2$), 1.40−1.07 (m, 60H, $C\underline{H}_2$); $^{13}C\{^1H\}$ 193.8 (t, $^2J_{PC}$ = 8.8 Hz, $\underline{C}O$ *trans* to CO), 190.3 (t, $^2J_{PC}$ = 8.4 Hz, $\underline{C}O$ *trans* to Cl), 160.9 (s, $\underline{C}_6H_4$ *p* to P), 136.0 (virtual t,[16] $^2J_{PC}$ = 6.0 Hz, $\underline{C}_6H_4$ *o* to P), 126.7 (virtual t,[16] $^1J_{PC}$ = 26.6 Hz, $\underline{C}_6H_4$ *i* to P), 114.6 (virtual t,[16] $^3J_{PC}$ = 5.3 Hz, $\underline{C}_6H_4$ *m* to P), 67.8 (s, $O\underline{C}H_2$), 30.0 (s, $\underline{C}H_2$), 29.7 (s, $\underline{C}H_2$), 29.5 (s, $\underline{C}H_2$), 29.3 (s, $\underline{C}H_2$), 29.1 (s, $\underline{C}H_2$), 26.1 (s, $\underline{C}H_2$); $^{31}P\{^1H\}$ 3.2 (s). IR (cm^{-1}, powder film): 2046 (m, ν_{CO}), 1937 (s, ν_{CO}), 1907 (s, ν_{CO}).

■ ASSOCIATED CONTENT

Supporting Information

The Supporting Information is available free of charge at https://pubs.acs.org/doi/10.1021/acs.inorgchem.2c02855.

Additional NMR and crystallographic data (PDF)

Accession Codes

CCDC 601307 and 601308 contain the supplementary crystallographic data for this paper. These data can be obtained free of charge via www.ccdc.cam.ac.uk/data_request/cif, or by emailing data_request@ccdc.cam.ac.uk, or by contacting The Cambridge Crystallographic Data Centre, 12 Union Road, Cambridge CB2 1EZ, UK; fax: +44 1223 336033.

■ AUTHOR INFORMATION

Corresponding Author

John A. Gladysz − *Department of Chemistry, Texas A&M University, College Station, Texas 77842-3012, United States;* orcid.org/0000-0002-7012-4872; Email: gladysz@mail.chem.tamu.edu

Authors

Alexander L. Estrada − *Department of Chemistry, Texas A&M University, College Station, Texas 77842-3012, United States*

Leyong Wang − *Institut für Organische Chemie and Interdisciplinary Center for Molecular Materials, Friedrich-Alexander-Universität Erlangen-Nürnberg, Erlangen 91054, Germany;* orcid.org/0000-0001-5775-3714

Gisela Hess − *Institut für Organische Chemie and Interdisciplinary Center for Molecular Materials, Friedrich-Alexander-Universität Erlangen-Nürnberg, Erlangen 91054, Germany*

Frank Hampel − *Institut für Organische Chemie and Interdisciplinary Center for Molecular Materials, Friedrich-Alexander-Universität Erlangen-Nürnberg, Erlangen 91054, Germany*

Complete contact information is available at: https://pubs.acs.org/10.1021/acs.inorgchem.2c02855

Notes

The authors declare no competing financial interest.

■ ACKNOWLEDGMENTS

The authors thank the U.S. National Science Foundation (Grants CHE-1566601 and CHE-1900549) for support.

■ REFERENCES

(1) Kottas, G. S.; Clarke, L. I.; Horinek, D.; Michl, J. Artificial Molecular Rotors. *Chem. Rev.* **2005**, *105*, 1281−1376.

(2) (a) Howe, M. E.; Garcia-Garibay, M. A. The Roles of Intrinsic Barriers and Crystal Fluidity in Determining the Dynamics of Crystalline Molecular Rotors and Molecular Machines. *J. Org. Chem.* **2019**, *84*, 9835−9849. (b) Jin, M.; Ando, R.; Jellen, M. J.; Garcia-Garibay, M. A.; Ito, H. Encapsulating *N*-Heterocyclic Carbene Binuclear Transition-Metal Complexes as a New Platform for Molecular Rotation in Crystalline Solid-State. *J. Am. Chem. Soc.* **2021**, *143*, 1144−1153.

(3) Tsuchiya, T.; Inagaki, Y.; Yamaguchi, K.; Setaka, W. Structure and Dynamics of Crystalline Molecular Gyrotops with a Difluorophenylene Rotor. *J. Org. Chem.* **2021**, *86*, 2423−2430 and earlier work cited therein..

(4) Ehnbom, A.; Gladysz, J. A. Gyroscopes and the Chemical Literature, 2002−2020: Approaches to a Nascent Family of Molecular Devices. *Chem. Rev.* **2021**, *121*, 3701−3750.

(5) (a) Lang, G. M.; Shima, T.; Wang, L.; Cluff, K. J.; Skopek, K.; Hampel, F.; Blümel, J.; Gladysz, J. A. Gyroscope-Like Complexes Based on Dibridgehead Diphosphine Cages That Are Accessed by Three-Fold Intramolecular Ring Closing Metatheses and Encase $Fe(CO)_3$, $Fe(CO)_2(NO)^+$, and $Fe(CO)_3(H)^+$ Rotators. *J. Am. Chem. Soc.* **2016**, *138*, 7649−7663. (b) Lang, G. M.; Skaper, D.; Hampel, F.; Gladysz, J. A. Synthesis, reactivity, structures, and dynamic properties of gyroscope like iron complexes with dibridgehead diphosphine cages: pre- *vs.* post-metathesis substitutions as routes to adducts with neutral dipolar Fe(CO)(NO)(X) rotors. *Dalton Trans.* **2016**, *45*, 16190−16204.

(6) (a) Nawara-Hultzsch, A. J.; Stollenz, M.; Barbasiewicz, M.; Szafert, S.; Lis, T.; Hampel, F.; Bhuvanesh, N.; Gladysz, J. A. Gyroscope-Like Molecules Consisting of PdX_2/PtX_2 Rotators within Three-Spoke Dibridgehead Diphosphine Stators: Syntheses, Substitution Reactions, Structures, and Dynamic Properties. *Chem. Eur. J.* **2014**, *20*, 4617−4637. (b) Kharel, S.; Joshi, H.; Bhuvanesh, N.; Gladysz, J. A. Syntheses, Structures, and Thermal Properties of Gyroscope-like Complexes Consisting of $PtCl_2$ Rotators Encased in Macrocyclic Dibridgehead Diphosphines $P((CH_2)_n)_3P$ with Extended Methylene Chains (n = 20/22/30), and Isomers Thereof. *Organometallics* **2018**, *37*, 2991−3000.

(7) See also: Zarcone, S. R.; Verardi, P. J.; Bhuvanesh, N.; Gladysz, J. A. A surprise landing on the *terra incognita* of macrocyclic dibridgehead diorganoarsines: syntheses, structures, and reactivities. *Chem. Commun.* **2022**, *58*, 8694−8697.

(8) Estrada, A. L.; Wang, L.; Bhuvanesh, N.; Hampel, F.; Gladysz, J. A. Syntheses, Structures, Reactivities, and Dynamic Properties of Gyroscope-like Complexes Consisting of Rh(CO)(X) or $Rh(CO)_2(I)$ Rotators and Cage-like *Trans* Aliphatic Dibridgehead Diphosphine Stators. *Organometallics* **2022**, *41*, 733−749.

(9) (a) Fiedler, T.; Bhuvanesh, N.; Hampel, F.; Reibenspies, J. H.; Gladysz, J. A. Gyroscope like molecules consisting of trigonal or square planar osmium rotators within three-spoked dibridgehead diphosphine stators: syntheses, substitution reactions, structures, and dynamic properties. *Dalton Trans.* **2016**, *45*, 7131−7147. (b) Hess, G. D.; Fiedler, T.; Hampel, F.; Gladysz, J. A. Octahedral Gyroscope-like Molecules Consisting of Rhenium Rotators within Cage-like Dibridgehead Diphosphine Stators: Syntheses, Substitution Reactions, Structures, and Dynamic Properties. *Inorg. Chem.* **2017**, *56*, 7454−7469.

(10) (a) Costello, J. F.; Davies, S. G.; Gould, E. T. F.; Thomson, J. E. Conformational analysis of triphenylphosphine ligands in stereogenic monometallic complexes: tools for predicting the preferred configuration of the triphenylphosphine rotor. *Dalton Trans.* **2015**, *44*, 5451−5466. (b) Brunner, H.; Tsuno, T. Comment on "Conformational analysis of triphenylphosphine ligands in stereogenic monometallic complexes: tools for predicting the preferred configuration of the triphenylphosphine rotor" by J. F. Costello, S. G. Davies, E. T. F. Gould and J. E. Thomson, Dalton Trans., 2015, 44, 5451. *Dalton Trans.* **2017**, *46*, 5103.

(11) Bauer, I.; Habicher, W. D. *In,out*-Isomerism of Phosphorus Bridgehead Cage Compounds. A Review. *Collect. Czech. Chem. Commun.* **2004**, *69*, 1195−1230.

(12) Däbritz, F.; Theumer, G.; Gruner, M.; Bauer, I. New conformational flexible phosphane and phosphane oxide macrobicycles. *Tetrahedron* **2009**, *65*, 2995−3002.

(13) Alder, R. W.; East, S. P. *In/Out* Isomerism. *Chem. Rev.* **1996**, *96*, 2097−2111.

(14) Wang, L.; Hampel, F.; Gladysz, J. A. "Giant" Gyroscope-Like Molecules Consisting of Dipolar Cl-Rh-CO Rotators Encased in Three-Spoke Stators That Define 25−27-Membered Macrocycles. *Angew. Chem., Int. Ed.* **2006**, *45*, 4372−4375 ("Gyroskop-Giganten": dipolare Cl-Rh-CO-Rotatoren, umgeben von Statoren aus drei Speichen 25- bis 27-gliedriger Makrocyclen. *Angew. Chem.* **2006**, *118*, 4479−4482).

(15) (a) Dunbar, K. R.; Haefner, S. C. Crystallographic Disorder in the Orthorhombic Form of $RhCl(CO)(PPh_3)_2$: Relevance to the Reported Structure of the Paramagnetic Impurity in Wilkinson's Catalyst. *Inorg. Chem.* **1992**, *31*, 3676−3679. (b) Ruwwe, J.; Martín-Alvarez, J. M.; Horn, C. R.; Bauer, E. B.; Szafert, S.; Lis, T.; Hampel, F.; Cagle, P. C.; Gladysz, J. A. Olefin Metatheses in Metal Coordination Spheres: Versatile New Strategies for the Construction of Novel Monohapto or Polyhapto Cyclic, Macrocyclic, Polymacrocyclic, and Bridging Ligands. *Chem. Eur. J.* **2001**, *7*, 3931−3950.

(16) The ^nJ values given for the virtual triplets represent the *apparent* couplings between adjacent peaks, not the mathematically rigorously coupling constants (*n* denotes the minimum number of bonds separating the interacting nuclei). Hersh, W. H. False AA′X Spin-Spin Coupling Systems in ^{13}C NMR: Examples Involving Phosphorus and a 20-Year-Old Mystery in Off-Resonance Decoupling. *J. Chem. Educ.* **1997**, *74*, 1485−1488.

(17) Siegel, J. S.; Anet, F. A. L. Dichlorofluoromethane-*d*: A Versatile Solvent for VT-NMR Experiments. *J. Org. Chem.* **1988**, *53*, 2629−2630.

(18) Bondi, A. van der Waals Volumes and Radii. *J. Phys. Chem.* **1964**, *68*, 441−451.

(19) (a) Takahashi, O.; Kohno, Y.; Nishio, M. Relevance of Weak Hydrogen Bonds in the Conformation of Organic Compounds and Bioconjugates: Evidence from Recent Experimental Data and High-Level *ab Initio* MO Calculations. *Chem. Rev.* **2010**, *110*, 6049−6076. (b) Tsuzuki, S.; Fujii, A. Nature and physical origin of CH/π interaction: significant difference from conventional hydrogen bonds. *Phys. Chem. Chem. Phys.* **2008**, *10*, 2584−2594.

(20) (a) Cetinkaya, B.; Lappert, M. F.; McMeeking, J.; Palmer, D. E. Unsaturated σ-Hydrocarbyl Transition-metal Complexes. Part I. Trimethyltin Acetylides as Sources of Late Transition-metal Derivatives: Metathesis, Oxidative Addition, and Oxidative Cleavage. *J. Chem. Soc., Dalton Trans.* **1973**, 1202−1208. (b) Weng, W.; Bartik, T.; Brady, M.; Bartik, B.; Ramsden, J. A.; Arif, A. M.; Gladysz, J. A. Synthesis, Structure, and Redox Chemistry of Heteropolymetallic Carbon Complexes with MC_2M', MC_4M', and $MC_4M'C_4M$ Linkages. Transmetalations of Lithiocarbon Complexes $(\eta^5\text{-}C_5Me_5)Re(NO)(PPh_3)(C{\equiv}CLi)$ and $(\eta^5\text{-}C_5Me_5)Re(NO)(PPh_3)(C{\equiv}CC{\equiv}CLi)$. *J. Am. Chem. Soc.* **1995**, *117*, 11922−11931.

(21) (a) Choi, J.-C.; Osakada, K.; Yamamoto, T. Single and Multiple Insertion of Arylallene into the Rh-H Bond to Give (π-Allyl)rhodium Complexes. *Organometallics* **1998**, *17*, 3044−3050. (b) For the analogous bis($PiPr_3$) complex, see: Schäfer, M.; Wolf, J.; Werner, H. Vinyliden-Übergangsmetallkomplexe XXX. Reaktionen von Acetato- und Trifluoracetato-Rhodium(I)-Komplexen mit 1-Alkinen: Ein Beispiel für die Balance zwischen isomeren π-Alkin-, Alkinyl(hydrido)- und Vinyliden-Metallverbindungen. *J. Organomet. Chem.* **1995**, *485*, 85−100.

(22) (a) This limit was computed using the experimental $\delta\nu$ value (108 Hz) per the worked example in the Supporting Information of the following study: (b) Lang, G. M.; Bhuvanesh, N.; Reibenspies, J. H.; Gladysz, J. A. Syntheses, Reactivity, Structures, and Dynamic Properties of Gyroscope-like Iron Carbonyl Complexes based on Dibridgehead Diarsine Cages. *Organometallics* **2016**, *35*, 2873−2889.

(23) Interestingly, as can be inferred from the views in Figure 1, the OC−Rh−P−C_{ipso} torsion angles of **6b** and **6c** [−3.4(2)° and 11.1(2)°; −7.0(4)° and 10.0(4)°] are very close to those in **XI** (i.e., CO ligand and macrocycle nearly eclipsed about the Rh−P bond). Perhaps **XI** can sometimes be a local minimum, closely straddled by two transition states, leading to **IX** and **X**.

(24) (a) Reimann, R. H.; Singleton, E. Transition metal carbonyls IV. Substitution reactions of rhenium pentacarbonyl bromide. *J. Organomet. Chem.* **1973**, *59*, 309−315. (b) Yamazaki, Y.; Morimoto, T.; Ishitani, O. Synthesis of novel photofunctional multinuclear complexes using a coupling reaction. *Dalton Trans.* **2015**, *44*, 11626−11635. (c) For complexes with phosphorus donor ligands that contain a terminal vinyl group, see: Álvarez-Pazos, N.; Bravo, J.; Graña, A. M.; García-Fontán, S. Rhenium(I) carbonyl complexes bearing the alkenylphosphinite ligand $Ph_2POCH_2CH = CH_2$. *Polyhedron* **2020**, *176*, 114288.

(25) Schmidt, S. P.; Trogler, W. C.; Basolo, F. Pentacarbonylrhenium Halides. *Inorg. Synth.* **1985**, *23*, 41−46.

(26) Adams, D. M. *Metal−Ligand and Related Vibrations*; Edward Arnold (Publisher) Ltd.: London, 1967, Chapter 3.

(27) Bond, A. M.; Colton, R.; McDonald, M. E. Chemical and Electrochemical Studies of Tricarbonyl Derivatives of Manganese and Rhenium. *Inorg. Chem.* **1978**, *17*, 2842−2847.

(28) It has been challenging to isolate **14c** and **14d** in analytically pure form, in part because of the usual issues in working with small quantities of air-sensitive substances at the ends of synthetic sequences involving several steps with moderate yields and stoichiometric steps in a precious metal. Thus, some of the spectroscopic experiments were carried out with samples of 90−95% purities.

(29) Boyd, S. E.; Field, L. D.; Hambley, T. W.; Partridge, M. G. Synthesis and Characterization of $Rh(P(CH_3)_3)_2(CO)CH_3$ and $Rh(P(CH_3)_3)_2(CO)Ph$. *Organometallics* **1993**, *12*, 1720−1724.

(30) Park, C. H.; Simmons, H. E. Macrobicyclic Amines. II. *out-out* ⇌ *in-in* Prototropy in 1,(k + 2)-Diazabicyclo[*k.l.m*] alkaneammonium Ions. *J. Am. Chem. Soc.* **1968**, *90*, 2429−2431. See also the immediately preceding and following communications in this issue.

(31) (a) Stollenz, M.; Barbasiewicz, M.; Nawara-Hultzsch, A. J.; Fiedler, T.; Laddusaw, R. M.; Bhuvanesh, N.; Gladysz, J. A. Dibridgehead Diphosphines that Turn Themselves Inside Out. *Angew. Chem., Int. Ed.* **2011**, *50*, 6647−6651 (Dreifach-verbrückte Diphosphane mit von innen nach außen invertierender Konfiguration. *Angew. Chem.* **2011**, *123*, 6777−6781). (b) Zhu, Y.; Stollenz, M.; Zarcone, S. R.; Kharel, S.; Hemant, J.; Bhuvanesh, N.; Reibenspiess, J. H.; Gladysz, J. A. Syntheses, Homeomorphic and Configurational Isomerizations, and Structures of Macrocyclic Aliphatic Dibrigehead Diphosphines: Molecules that Turn Themselves Inside Out. *Chem. Sci.* **2022**, *13*, DOI: 10.1039/D2SC94724A.

(32) (a) Haines, A. H.; Karntiang, P. Synthesis of Some out,in- and out,out-Macrobicyclic Polyethers derived from Glycerol. Out,in-in,out Isomerism. *J. Chem. Soc. Perkin Trans. 1* **1979**, 2577−2587. (b) Wareham, R. S.; Kilburn, J. D.; Turner, D. L.; Rees, N. H.; Holmes, D. S. Homeomorphic Isomerism in a Peptidic Macrobicycle. *Angew. Chem., Int. Ed. Engl.* **1996**, *34*, 2660−2662 (Homöomorphe Isomerie in einem Peptid-Makrobicyclus. *Angew. Chem.* **1995**, *107*, 2902−2904). (c) Saunders, M.; Krause, N. The Use of Stochastic Search in Looking for Homeomorphic Isomerism: Synthesis and Properties of Bicyclo[6.5.1]-tetradecane. *J. Am. Chem. Soc.* **1990**, *112*, 1791−1795. (d) Alder, R. W.; Heilbronner, E.; Honegger, E.; McEwen, A. B.; Moss, R. E.; Olefirowicz, E.; Petillo, P. A.; Sessions, R. B.; Weisman, G. R. The *out,out* to *out,in* Transition for 1,(n+2)-Diazabicyclo[n.3.1]alkanes. *J. Am. Chem. Soc.* **1993**, *115*, 6580−6591. (e) Wang, X.; Shyshov, O.; Hanževački, M.; Jäger, C. M.; von Delius, M. Ammonium Complexes of Orthoester Cryptands Are Inherently Dynamic and Adaptive. *J. Am. Chem. Soc.* **2019**, *141*, 8868−8876. (f) Löw, H.; Mena-Osteritz, E.; Mullen, K. M.; Jäger, C. M.; Delius, M. Self-Assembly, Adaptive Response, and *in,out*-Stereoisomerism of Large Orthoformate Cryptands. *ChemPlusChem.* **2020**, *85*, 1008−1012.

(33) Baechler, R. D.; Mislow, K. The Effect of Structure on the Rate of Pyramidal Inversion of Acyclic Phosphines. *J. Am. Chem. Soc.* **1970**, *92*, 3090−3093.

(34) (a) Barder, T. E.; Buchwald, S. L. Rationale Behind the Resistance of Dialkylbiaryl Phosphines toward Oxidation by Molecular

Oxygen. *J. Am. Chem. Soc.* **2007**, *129*, 5096−5101. (b) Stewart, B.; Harriman, A.; Higham, L. J. Predicting the Air Stability of Phosphines. *Organometallics* **2011**, *30*, 5338−5343.
(35) (a) Buchmeiser, M. R. Catalysis in Confined Spaces. *ChemCatChem.* **2021**, *13*, 785−786. This article introduces a thematic issue devoted to this topic. (b) Jans, A. C. H.; Caumes, X.; Reek, J. N. H. Gold Catalysis in (Supra)Molecular Cages to Control Reactivity and Selectivity. *ChemCatChem.* **2019**, *11*, 287−297.
(36) Jung, M. E.; Piizzi, G. *gem*-Disubstituent Effect: Theoretical Basis and Synthetic Applications. *Chem. Rev.* **2005**, *105*, 1735−1766.
(37) Friedrichsen, B. P.; Powell, D. R.; Whitlock, H. W. Sterically Encumbered Functional Groups: An Investigation of Endo versus Exo Phosphoryl Complexation Using ^{1}H and ^{31}P NMR. *J. Am. Chem. Soc.* **1990**, *112*, 8931−8941.
(38) Zarcone, S. R.; Gladysz, J. A. Manuscript in preparation.
(39) These assignments were confirmed by ^{1}H,^{1}H COSY and ^{1}H,^{13}C COSY experiments.
(40) Although some compounds did not give satisfactory microanalyses, the best available data are given.
(41) The **C**O signal was not observed.
(42) The $\underline{C}\equiv\underline{C}$ $^{13}C\{^{1}H\}$ NMR signals of *trans*-Rh(CO)(C≡CC$_6$H$_5$)(PPh$_3$)$_2$ appear at 123.7 and 125.1 ppm (C$_6$D$_6$; $\Delta\delta$ = 1.4 ppm),[21a] so the unresolved 121.5−121.3 ppm signal of **7b** is tentatively assigned to both sp carbon atoms. One or both C≡C signals of **8b** are tentatively assigned to a 121.6−121.3 signal (the sample also exhibits a weak 136.4 ppm signal, believed to be an impurity).
(43) The J_{PC} coupling was not observed.
(44) These signals were more intense than the others (ca. 2:1).

https://doi.org/10.1021/acs.inorgchem.2c02855
Inorg. Chem. 2022, 61, 17012−17025